Title
Mitochondrial Fission in Pancreatic Beta Cell Insulin Secretion

Author
Hennings, Thomas George

Publication Date
2018

Peer reviewed|Thesis/dissertation

Mitochondrial Fission in Pancreatic Beta Cell Insulin Secretion

by

Thomas George Hennings

DISSERTATION

Submitted in partial satisfaction of the requirements for the degree of

DOCTOR OF PHILOSOPHY

in

Biomedical Sciences

in the

GRADUATE DIVISION

of the

UNIVERSITY OF CALIFORNIA, SAN FRANCISCO

Committee in Charge

To my partner, Lindsey Elise Jones.

For her unending support, encouragement, and love. You are my rock.

ACKNOWLEDGEMENTS

I am fortunate that my time in the Biomedical Sciences program at UCSF has been filled with great friends, supportive mentors, and exciting accomplishments - all of which helped me achieve a tremendous amount of both personal and professional growth.

No one has been more instrumental in my development than my advisor and mentor, Dr. Gregory Ku. I was initially drawn to work with Greg due to this ability to conceptualize and execute clever experiments that appeal to a broad audience within the diabetes field. As a mentor, Greg both pushed me to become an independent thinker but didn't hesitate to "jump in the trenches" with me when I needed a little extra guidance – there was more than one instance when Greg was at the bench with me pipetting away. Greg is a thoughtful, down-to-earth scientist who is willing and eager to think outside the box and lend his time to help others. I will always admire Greg's deep passion for generating new data, his unending goodwill towards others and his unwavering optimism. Thank you, Greg, for everything you have done to help me develop into the person and scientist that I am today. I am lucky to have trained under your guidance and will carry with me the lessons you taught me for the rest of my life.

Apart from my advisor, my thesis committee members Dr. Michael German and Dr. Julie Sneddon have been instrumental in my development as a scientist. Mike has been an unending source of helpful insights about diabetes and science in general. I have never been so amazed at one person's ability to ask such pointed and insightful comments during scientific presentations, often without having witnessed the supporting background material. Julie has been an excellent role model of that rare combination of a sharp intellect and infectious charisma. Every time I have watched Julie give a scientific presentation, I have been impressed by both the precision and ambition of her research, and her engaging and articulate presentation style. I hope to someday have the opportunity to be a knowledge resource and role model to aspiring professionals in the same way that Mike and Julie have been for me.

I have been fortunate to work with a large number of hard-working, thoughtful, colleagues in the UCSF Diabetes Center. To all of the Diabetes Center technicians, graduate students, and postdocs that I have had the pleasure of getting to know over these last six years; thank you for your camaraderie, and I hope our paths cross again in the future. To Dr. Holger Russ, thank you for showing me how to channel passion into productivity, and for believing in a bright-eyed first year graduate student with unending enthusiasm for diabetes. In many ways, my time working with you was the most formative of these past six years. I will always think of you as an example of how to thoroughly enjoy your work, while simultaneously holding yourself to a tremendously high standard and inspiring others to do the same. To UCSF professor emeritus Dr. Gerold Grodsky, thank you for sharing with me your unending enthusiasm for science. I am very privileged to have been able to work with and get to know one of the founders of the field of insulin secretion, who has dedicated so much of his own time and effort to help the diabetes field develop into what it is today. To Vi Dang, Vinh Nguyen, and Gregory Szot in the UCSF Islet Production Core, thank you for your willingness to perform islet isolations on my mice at short notice and at odd hours. The vast majority of my experiments would not have been possible without the pancreatic islet isolations completed with your expert assistance. To Christophe Paillart, the Diabetes Center facility manager, thank you for being willing and enthusiastic to help with the myriad of challenges that inevitably arise when doing research. From troubleshooting the Seahorse machine to finding a wrench that fits the oxygen regulator, if no one else knows what to, then a text to Christophe usually revealed the answer. To Lily Yu, Karyl Nakamura, and Jimmy Chen, thank you for your endless patience when listening to my numerous questions about the non-technical aspects of doing research. You are the oil that keeps this research machine running smoothly, and we would all be truly lost without you. A special thank you to Jimmy Chen for his endlessly entertaining and insightful seminar announcement illustrations. Whenever I was having a rough day, I knew that I could count on reading through one of Jimmy's announcements for a laugh and a dose of perspective. Jimmy, you are a maverick. Never stop.

I would never have had the opportunity to learn and grow here at UCSF without the wonderful environment and community created and fostered by the Biomedical Sciences graduate program. I extend my sincerest thanks to all of the BMS administrators. A special thank you to Lisa Magargal and her meticulously thoughtful, student-focused organization of the program during her tenure as program administrator, and to Demian Sainz for continuing and expanding on this approach when he took over as administrator. Demian is the foundation of BMS and the main force in helping shape the direction of our program. Thank you for putting the needs and concerns of students first, and for being so responsive to changes and improvements that are suggested by students. To all of the BMS students that I have had the pleasure of getting to know over the years: I will treasure our memories together, and look forward to more adventures in the future.

A few of my friends deserve specific shout-outs: First, to Derek Bissell, thank you for being such a loyal friend through all of life's adventures, and for making growing up a nerdy, awkward goofball much less lonely; to Thompson Sowash, thank you for teaching me how to always see the brighter side of life and constantly encouraging me to follow my passion for diabetes; to Mark Keating, thank you for reminding me to go outside once in a while and sharing your gummy vitamins with me; to Aaron Mattingly, thank you for always being there for me, and for helping me realize that there are people out there who are much funnier than I am (i.e. you); to Dan Holohan, thank you for being my career exploration wingman, and for always dancing like no one is watching; to KT Nguyen, thank you for understanding my perspective as only a fellow little-brother can, and for helping foster and expand my love of meat; to Drew McKinney and Adrienne Stormo, thank you for letting me become a cat uncle, and for sharing my passion for random geography facts.

I am very fortunate to have grown up in a family with abundant love that valued and encouraged my individuality. To my mother, Darlene Hennings, thank you for teaching me honesty and compassion, and for raising me to believe that I can achieve whatever I set my mind

to. To my father, David Hennings, thank you for teaching me how to think analytically, and always encouraging and enabling me to pursue my interests and passions, however reckless they may be. To my sister, Rebecca Rapp, thank you for putting up with my endless little-brother shenanigans throughout our childhood and for constantly being a role model of how to be a good, honest person. To my brother in law, Jason Rapp, thank you for reminding me to stand up for myself when I know that I am correct. And finally, to my nephew Levi “Blaze” Rapp, thank you for reinvigorating my desire to make the world a better place.

Last but certainly not least is my partner Lindsey Jones, who played an absolutely crucial role in helping me arrive to this point. Lindsey has been by my side through all of the ups and downs of graduate school. Thank you for all the evening lab dinner deliveries, sharing my passion for tacky holiday sweaters, and loving me both despite and because of all my endearing contradictions. Thank you for being my cheerleader, my co-conspirator, my rock, my partner, and my best friend. I could not have done this without you. I am so proud of all that we have achieved together, and I can’t wait to see what life as doctors has in store for us.

CONTRIBUTIONS TO THE PRESENTED WORK

The work described in this dissertation was performed under the direct supervision and guidance of Dr. Gregory M. Ku, M.D., Ph.D. Additional guidance and insight were provided by thesis committee members Dr. Michael S. German, M.D., and Dr. Julie B. Sneddon, Ph.D.

Chapters 2 and 3 are reprinted largely as they appear in:

Hennings TG, Chopra DG, DeLeon ER, VanDeusen HR, Sesaki H, Merrins MJ, Ku GM. In Vivo Deletion of β-Cell Drp1 Impairs Insulin Secretion Without Affecting Islet Oxygen Consumption. Endocrinology. doi: 10.1210/en.2018-00445.

Mitochondrial Fission in Pancreatic Beta Cell Insulin Secretion

Thomas George Hennings

ABSTRACT

Insulin-producing pancreatic beta cells are central regulators of blood glucose homeostasis. In a process termed glucose-stimulated insulin secretion (GSIS) beta cells utilize mitochondrial glucose metabolism to precisely up- or down-regulate insulin vesicle exocytosis in response to changes in plasma glucose concentrations. As beta cells either die or become dysfunctional in both type 1 and type 2 diabetes, they are an attractive target for the generation of novel therapeutics. To discover new genetic regulators of beta cell biology, we conducted a genome-wide screen of beta cell insulin production and identified an important role for mitochondrial fission genes. Mitochondrial fission, the process by which one parental mitochondrion gives rise to multiple daughter mitochondria, regulates ATP production, the tricarboxylic acid (TCA) cycle, and processes beyond metabolism in a cell-type specific manner. Given the central role of mitochondrial metabolism in GSIS, we hypothesized that mitochondrial fission may play an important role in regulating beta cell insulin secretion. We thus generated mice lacking beta cell Drp1 (Drp1β-KO mice), a central regulator of mitochondrial fission. We found that Drp1β-KO mice were glucose intolerant due to impaired GSIS, but did not progress to fasting hyperglycemia as adults. Despite markedly abnormal mitochondrial morphology, Drp1β-KO islets exhibited normal oxygen consumption rates and an unchanged glucose threshold for intracellular calcium mobilization. Instead, the most profound consequences of beta cell Drp1 deletion were impaired second-phase insulin secretion and impaired glucose-stimulated amplification of insulin secretion. Our data establish Drp1 as an important regulator of insulin secretion *in vivo*, and demonstrate a novel role for Drp1 in metabolic amplification and calcium handling without affecting oxygen consumption. Future studies will investigate the contribution of abnormal mitochondrial dynamics to the development of diabetes.

Table of Contents

LIST OF FIGURES

CHAPTER 1: INTRODUCTION

1.1 Pancreatic Beta Cells and Diabetes Mellitus

Pancreatic beta cells, located within clusters of endocrine cells known as Islets of Langerhans, are the only cell type in the body capable of producing physiological amounts of the glucose-lowering hormone insulin. Death or dysfunction of beta cells contributes to the pathogenesis of most types of diabetes mellitus, a group of diseases characterized by hyperglycemia (abnormally elevated blood glucose concentrations). The most common variants are type 1 diabetes, an autoimmune condition in which pancreatic beta cells are selectively destroyed, and type 2 diabetes, a metabolic condition characterized first by insulin resistance and ultimately by beta cell death and dysfunction.

In a non-diabetic individual, though a process termed glucose-stimulated insulin secretion (GSIS) beta cells upregulate insulin vesicle exocytosis upon exposure to elevated glucose and then promptly downregulate insulin secretion once again when glucose levels return to baseline. This precise control over insulin secretion is crucial – while inadequate insulin secretion can produce hyperglycemia and contribute to diabetes, excess insulin can cause blood glucose levels to drop abnormally low (hypoglycemia) which can be life-threatening if not promptly reversed. Beta cells utilize a complex set of cell biological processes to achieve GSIS. Mitochondrial metabolism of glucose plays a key role by allowing changes extracellular glucose concentrations to be translated into increased intracellular ATP, which in GSIS acts as a second messenger to trigger additional events that ultimately culminate in insulin vesicle exocytosis. A number of points within the GSIS cascade have been found to be dysfunctional in beta cells from patients with type 2 diabetes.

Substantial research has been directed towards understanding the mechanisms underlying beta cell death and dysfunction in diabetes, as well as into identifying different pathways that can be targeted to overcome these pathologies. There have been a number of notable successes: two classes of widely used drugs in T2D (sulfonylureas and GLP1 receptor agonists) act primarily on the beta cell to augment insulin secretion in response to challenge with

elevated glucose concentrations, and in T1D a recent study[1] and clinical trial (NCT02372253) identified a beneficial role for the calcium channel blocker verapamil in preserving beta cell function and mass shortly after diagnosis. Unfortunately, these therapies, along with other approaches to treat diabetes, are not sufficient to reverse hyperglycemia in many T2D patients or to irreversibly alter disease progression in T1D. Novel approaches to preventing and treating diabetes are thus greatly needed.

1.2 Novel Genetic Regulators of Beta Cell Function

In order to identify novel genetic regulators of beta cell biology, we recently conducted a genome-wide siRNA screen of insulin expression[2]. The results of this screen both confirmed the known functions of transcription factors such as Glis3, Pdx1, and NeuroD1 in regulating insulin expression, and identified a number of novel genes regulating insulin expression. For example, we identified Spry2, a modulator of receptor tyrosine kinase activity and T2D genome-wide association study hit, as a regulator of insulin expression through modulation of the unfolded protein response. The screen also identified a number of mitochondrial genes as regulators of insulin expression, including components of the electron transport chain (ETC; Atp5a1, Atp5j2, Cox6b1, Cox6c, and Cox7a2), and several mitochondrial dynamics genes (Mid51, Mff, and 4930550C14Rik, later named Mfi[3]). Mitochondrial dynamics is an umbrella term that includes the interrelated processes of mitochondrial fission, mitochondrial fusion, and mitochondrial autophagy (mitophagy). Mitochondrial dynamics has been found regulate as diverse cellular processes as oxidative phosphorylation, axonal mitochondrial transport, mitochondrial DNA replication, and reactive oxygen species production, among others[4].

Interestingly, all of the mitochondrial dynamics genes identified in our screen of insulin expression encode mitochondrial fission proteins. Mitochondrial fission is the process by which one mitochondrion gives rise to multiple daughter mitochondria. In a normal cell, exposure to a pro-fission stimulus causes the dynamin-related GTPase Drp1 to translocate from the cytosol to

the mitochondria, where it binds to one of four receptor proteins (Fis1, MiD49, MiD51, and Mff). Upon binding, Drp1 oligomerizes to encircle and constrict the mitochondria. The daughter mitochondria then separate at the site of constriction, potentially due to the action of a second dynamin-related GTPase, Dyn2[5].

1.3 Aims of This Study

In the pancreatic beta cell, the role of mitochondrial fission remains largely unexplored. Past efforts to characterize the roles of mitochondrial fission genes have largely been conducted *in vitro* in immortalized beta cell lines that likely do not reflect the metabolic milieu that beta cells experience *in vivo*[6–8]. Thus, the aims of this study were first, to investigate the role of pancreatic beta cell mitochondrial fission *in vivo*, and second to more clearly define the role of mitochondrial fission in pancreatic beta cell insulin secretion. Both of these aims were selected with the ultimate goals of 1) identifying novel pathways that can be targeted in diabetes for therapeutic benefit, 2) uncovering knowledge that contributes to our understanding of beta cell death or diabetes pathogenesis.

CHAPTER 2: *In vivo* Deletion of Beta Cell Drp1 Impairs Insulin Secretion without Affecting Islet Oxygen Consumption

Content in this chapter was modified from the following publication:

Hennings TG, Chopra DG, DeLeon ER, VanDeusen HR, Sesaki H, Merrins MJ, Ku GM. In Vivo Deletion of β-Cell Drp1 Impairs Insulin Secretion Without Affecting Islet Oxygen Consumption. Endocrinology. 2018 Sep 1;159(9):3245-3256. doi: 10.1210/en.2018-00445.

2.1 ABSTRACT

Mitochondria are dynamic organelles that undergo frequent fission and fusion events. Mitochondrial fission is required for ATP production, the tricarboxylic acid (TCA) cycle, and processes beyond metabolism in a cell-type specific manner. *Ex vivo* and cell line studies have demonstrated that Drp1, a central regulator of mitochondrial fission, is required for glucose stimulated insulin secretion (GSIS) in pancreatic beta cells. Herein, we set out to interrogate the role of Drp1 in beta cell insulin secretion *in vivo*. We generated beta cell-specific Drp1 knockout (Drp1β-KO) mice by crossing a conditional allele of Drp1 to *Ins1*^{cre} mice, in which Cre recombinase replaces the coding region of the *Ins1* gene. We found that Drp1β-KO mice were glucose intolerant due to impaired GSIS, but did not progress to fasting hyperglycemia as adults. Despite markedly abnormal mitochondrial morphology, Drp1β-KO islets exhibited normal oxygen consumption rates and an unchanged glucose threshold for intracellular calcium mobilization. Instead, the most profound consequences of beta cell Drp1 deletion were impaired second-phase insulin secretion and impaired glucose-stimulated amplification of insulin secretion. Our data establish Drp1 as an important regulator of insulin secretion *in vivo*, and demonstrate a novel role for Drp1 in metabolic amplification and calcium handling without affecting oxygen consumption.

2.2 INTRODUCTION

Glucose-stimulated insulin secretion (GSIS) from pancreatic beta cells is comprised of interdependent pathways coupling glucose metabolism to insulin vesicle exocytosis[9–11]. In the triggering pathway, glucose metabolism produces an increase in the cytosolic ATP/ADP ratio, which triggers the closure of ATP-sensitive K^+ (K_{ATP}) channels and the opening of voltage-gated Ca^{2+} channels. The resulting influx of Ca^{2+} signals the exocytotic machinery to initiate insulin vesicle fusion with the plasma membrane. The metabolic amplifying pathways (previously termed the K_{ATP}-independent pathways) are responsible for the glucose-dependent increase in insulin

secretion that occurs when cytosolic Ca^{2+} is already elevated[9–11]. As mitochondria are central to both the triggering and amplifying pathways, healthy beta cell mitochondria are of upmost importance to glucose homeostasis[12].

The interdependent processes of mitochondrial fusion and fission represent an important, albeit incompletely understood, level of metabolic regulation. Disrupting the balance between fission and fusion has been shown to affect the tricarboxylic acid (TCA) cycle, oxygen consumption, ATP and reactive oxygen species (ROS) production, and mitochondrial processes beyond metabolism in various cell types[4]. Mitochondrial fission and fusion are themselves regulated by diverse stimuli, including cellular energy balance, proliferation, and mitochondrial function, among others, thus establishing a dynamic bi-directional feedback loop between cellular metabolism and mitochondrial morphology[4].

Previous studies examining the *in vivo* consequences of impairing beta cell mitochondrial fusion, either directly through the knockout of the fusion protein Opa1[13] or indirectly through deletion of prohibitin[14], reported profound mitochondrial defects that impaired insulin secretion through defective glucose-stimulated ATP production. *Ex vivo,* knockdown[6–8] or chemical inhibition of Drp1, a dynamin-related GTPase required for mitochondrial fission [7], have also been found to impair GSIS and ATP-linked oxygen consumption. However, these *ex vivo* studies may be confounded by the recently discovered off-target effect of the Drp1 inhibitor mDivi-1 on Complex I of the electron transport chain (ETC)[15]. Thus, it is not clear whether the consequences of blocking beta cell mitochondrial fission have been fully realized, especially as *in vivo* studies have not been performed.

Here, we generated a mouse model in which Drp1 is selectively deleted in pancreatic beta cells (Drp1β-KO mice). We show that Drp1β-KO mice are glucose intolerant due to impaired GSIS, and despite markedly abnormal mitochondrial morphology, Drp1β-KO islets exhibit normal oxygen consumption rates and an unchanged glucose threshold for intracellular

calcium mobilization. Instead, the most profound consequence of beta cell Drp1 deletion appears to be the impaired glucose-stimulated amplification of insulin secretion.

2.4 RESULTS

2.4.i Drp1β-KO mice are glucose intolerant

To generate mice selectively lacking beta cell Drp1, we crossed mice carrying a conditional allele of Drp1[16] to *Ins1*^{cre} mice in which Cre recombinase replaces the coding region of the *Ins1* gene[17]. We thus generated mice with wild-type beta cell Drp1 (Drp1β-WT), heterozygous Drp1 knockout (Drp1β-Het) and homozygous Drp1 knockout (Drp1β-KO). Drp1 protein was nearly undetectable in Drp1β-KO islets, and was reduced by ~50% in Drp1β-Het islets (Figure 2.1 A-B). As in other models of Drp1 knockdown[6–8], we found that Drp1β-KO beta cells contained a large perinuclear mitochondrial structure, with occasional linear and circular protrusions, consistent with a super-fused mitochondrial network (Figure 2.1 C, Figure 2.2). In contrast, Drp1β-WT mitochondria were networked diffusely throughout the cytoplasm, while Drp1β-Het beta cell mitochondria largely resembled -WT controls. Levels of other mitochondrial fission and fusion proteins were unchanged (Figure 2.3 A-G). Drp1β-KO beta cells also displayed elongated peroxisomes compared to the spherical peroxisomes of Drp1β-WT beta cells (Figure 2.3 H), consistent with the known role of Drp1 in peroxisomal fission[18–20].

At 8-12 weeks of age both male and female Drp1β-KO mice were hyperglycemic at 30, 60, 90, and 120 minutes after intraperitoneal glucose injection and by area under the curve (AUC) analysis (Figure 2.1 D-G) compared to Drp1β-WT mice. Drp1β-Het mice were not significantly different from Drp1β-WT mice by either method. At 30 weeks of age female Drp1β-KO mice were more glucose intolerant than at 8-12 weeks (Figure H-I). However, fasting blood glucose (Figure 2.1 J) and random blood glucose (Figure 2.4 A), at ages up to 30 weeks were not significantly changed. Insulin tolerance was also unchanged (Figure 2.4 B). After 12 weeks of high fat diet

(HFD, starting at 10 weeks of age), female Drp1β-KO mice were again glucose intolerant (Figure 2.4 C-D) but still did not develop fasting hyperglycemia. HFD did not change glucose tolerance in Drp1β-Het mice compared to Drp1β-WT controls. We note, however, that the effect of the *Ins1*^{cre} allele on glucose tolerance in high-fat diet (HFD) conditions has not been determined. These results indicate that the loss of beta cell Drp1 results in glucose intolerance without fasting hyperglycemia.

2.4.ii Drp1β-KO islets exhibit impaired GSIS and mitochondrial abnormalities

To explore the cause of Drp1β-KO glucose intolerance we assayed insulin secretion *in vivo*. Male Drp1β-KO mice showed reduced plasma insulin concentrations 15 minutes after intraperitoneal glucose injection compared to Drp1β-WT controls (Figure 2.5 A). Immunostaining for insulin and glucagon revealed no striking differences in islet architecture between Drp1β-KO and Drp1β-WT mice (Figure 2.4 E). *Ex vivo*, male Drp1β-KO islets secreted less insulin in response to stimulation with 16.7mM glucose than Drp1β-WT islets, with no change in response to 2.8mM glucose (Figure 2.5 B). Secretion in response to KCl at 2.8mM glucose was unchanged (Figure 2.5 C), suggesting that Drp1 deletion impaired GSIS upstream of plasma membrane depolarization. The insulin content of isolated Drp1β-KO islets was unchanged (Figure 2.5 D), indicating that the GSIS defect was not due to lack of insulin production. We thus hypothesized that the Drp1β-KO GSIS defect arose in the mitochondria.

Studies in cardiomyocytes have shown a correlation between Drp1 expression and ETC complex levels[21,22]. Indeed, we found that NDUFB8, SDHB, and ATP5A, components of ETC Complexes I, II, and IV respectively, were reduced in Drp1β-KO islets (Figure 2.5 E-J). UQCRC2 (Complex III) was non-significantly reduced (p=0.13) while MTCO1 (Complex V) was unchanged by Drp1 deletion. We next used 2-photon imaging of NADH and NADPH (collectively termed NAD(P)H) to directly image beta cell metabolism[23,24]. As expected from the mitochondrial morphology images in Figure 2.1 C, the NAD(P)H fluorescence in live Drp1β-WT beta cells was

distributed throughout the cytoplasm while the NAD(P)H fluorescence in Drp1β-KO beta cells was clustered in a perinuclear location (Figure 2.5 K). Quantification of these NAD(P)H images revealed that Drp1β-KO islets exhibited elevated NAD(P)H fluorescence at 2mM glucose and reduced NAD(P)H at 10mM glucose when compared to Drp1β-WT islets (Figure 2.5 L). NADPH levels measured using a bioluminescence-based method were unchanged between Drp1β-WT and -KO islets 15min after glucose stimulation (Figure 2.5 M). These observations raise the question of whether abnormal mitochondrial metabolism contributes to defective Drp1β-KO GSIS.

2.4.iii Beta cell Drp1 deletion does not affect islet oxygen consumption or the glucose threshold for islet calcium entry

To ascertain if Drp1β-KO islet mitochondrial abnormalities translate into impaired flux through the electron transport chain, we measured oxygen consumption rates (OCRs) in intact Drp1β-KO islets. Surprisingly, oxygen consumption by Drp1β-KO islets was indistinguishable from Drp1β-WT islets in response to sequential stimulation with 9mM glucose, 16.7mM glucose and the mitochondrial poisons oligomycin and rotenone/antimycin A (Figure 2.6 A). As such, there were no significant changes in ATP-linked respiration (Figure 2.6 B), basal respiration (Figure 2.6 C), proton leak (Figure 2.6 D), or coupling efficiency (Figure 2.6 E). In contrast to the upregulation of *Slc2a2* mRNA observed in Drp1-knockdown MIN6 cells[7], we found that mRNA expression of Glut2 (*Slc2a2*) and *Gck* were unchanged in Drp1β-KO islets (Figure 2.6 F). These data indicate that, surprisingly, respiration in Drp1β-KO islets is normal despite lower ETC component expression and abnormal NAD(P)H levels.

Downstream of metabolism-dependent K_{ATP} channel closure, an acute spike in cytosolic Ca^{2+} is required to trigger insulin secretion, and persistently elevated cytosolic Ca^{2+} is necessary to sustain secretion. Normal oxygen consumption in Drp1β-KO islets would be expected to produce a pattern of cytosolic Ca^{2+} elevation that is similar to that of Drp1β-WT islets. Therefore, we imaged islet cytosolic Ca^{2+} influx across a range of glucose concentrations (2-9mM) (Figure

2.6 G) in Drp1β-WT and Drp1β-KO islets. Average cytosolic Ca^{2+} was elevated at 2mM and 5mM glucose in Drp1β-KO islets, but both Drp1β-WT and -KO islets showed a robust "phase 0" in response to 5mM glucose, reflecting Ca^{2+} uptake by the endoplasmic reticulum[25]. Both Drp1β-WT and -KO islets exhibited an acute increase in cytosolic Ca^{2+} in response to 7mM glucose, indicating the glucose threshold required to trigger cytosolic Ca^{2+} influx was unchanged by Drp1 deletion. Likewise, islets of both genotypes exhibited a spike in cytosolic Ca^{2+} upon exposure to 9mM glucose. However, at 9mM glucose, average cytosolic Ca^{2+} in Drp1β-KO islets then decreased to a level lower than that of Drp1β-WT.

On the level of the individual islet, oscillations in cytosolic Ca^{2+} during glucose exposure cause pulses of insulin secretion[26]. Individual Drp1β-WT and -KO islet Ca^{2+} traces showed aperiodic depolarizations at 7mM glucose and exhibited robust oscillations at 9mM glucose (Figures 3H). Surprisingly, the Ca^{2+} oscillation period was nearly doubled in Drp1β-KO islets (Figure 2.6 I), with a concomitant reduction in oscillation amplitude, calculated as the difference between Ca^{2+} peak and nadir (Figure 2.6 J). However, the duty cycle, calculated as the fraction of time that an individual islet spends with cytosolic Ca^{2+} levels above half maximal, was unchanged in Drp1β-KO islets at 9mM glucose (Figure 2.6 K), again consistent with a normal threshold for glucose-stimulated cytosolic calcium increase[24,26]. These results show that Drp1β-KO islets have abnormal Ca^{2+} handling.

2.4.iv Loss of beta cell Drp1 impairs second phase insulin secretion and metabolic amplification

To look more closely at the effects of Drp1 deletion on insulin secretion, we measured insulin secretion dynamically using an islet perifusion assay. While first-phase insulin secretion was indistinguishable between Drp1β-WT and Drp1β-KO islets, second-phase insulin secretion was clearly impaired in Drp1β-KO islets (Figure 2.7 A). KCl-induced secretion at 2.8mM glucose was also unchanged, consistent with our results from static GSIS assays (Figure 2.5 C). AUC analysis of the perifusion curve confirmed these findings: total AUC and AUC during second

phase were reduced in Drp1β-KO islets (Figure 2.7 B and D), while first phase AUC (Figure 2.7 C) and KCl-induced AUC (Figure 2.7 E) were unchanged.

Independent of ATP-production and GSIS triggering, a number of glucose-derived mitochondrial metabolites influence insulin secretion through the metabolic amplifying pathway[26]. We measured the metabolic amplification of insulin secretion in Drp1β-WT and Drp1β-KO islets by treating them with either 2.8mM or 16.7mM glucose in the presence of KCl (30mM) and the K_{ATP} channel activator diazoxide (Dz, 200uM)[9–11]. At 2.8mM glucose, there was no difference between the genotypes, but at 16.7mM glucose Drp1β-KO islets displayed reduced insulin secretion compared to Drp1β-WT islets (Figure 2.7 F), reflecting impaired metabolic amplification.

2.5 DISCUSSION AND CONCLUSIONS

Herein we describe the first *in vivo* knockout of a mitochondrial fission protein in the pancreatic beta cell. Our study corroborates previous *in vitro* studies that identified a reduction in GSIS upon loss of beta cell Drp1, and expands the known roles of beta cell Drp1 with our findings of impaired second phase insulin secretion, abnormal islet Ca^{2+} handling, and defective metabolic amplification in Drp1β-KO islets.

We found that Drp1β-KO islet mitochondria were abnormal in several ways, exhibiting a highly fused morphology, decreased expression of ETC complexes, and altered NAD(P)H fluorescence at both low and high glucose. Nonetheless, Drp1β-KO islet oxygen consumption was unchanged, suggesting that Drp1β-KO islets retain adequate ETC expression to maintain normal mitochondrial oxidative phosphorylation and highlight the pitfall of using expression level to infer enzymatic activity[27]. Normal oxygen consumption is consistent with our unchanged threshold for glucose-stimulated cytosolic Ca^{2+} increase (Figure 2.6 G) and duty cycle measurements in Drp1β-KO islets (Figure 2.6 K). There is precedence for these observations: Drp1 deletion in primary fibroblasts and macrophages also does not impair oxygen

consumption[28–30]. Importantly, our data do show that there is a triggering pathway defect in Drp1β-KO islets, just not at the level of the electron transport chain. Average Ca^{2+} levels are elevated at 2mM and 5mM glucose and reduced at 9mM glucose after a normal initial rise. These changes in cytosolic Ca^{2+} could represent accommodation to a narrowed functional range of the triggering pathway components or a primary defect in Ca^{2+} handling caused by Drp1 loss. Although there are no reported links between elongated peroxisomes and insulin secretion, given the parallel role of Drp1 in peroxisomal fission[18–20] we also cannot rule out non-mitochondrial contributions to the Drp1β-KO GSIS defect. Future studies are needed to distinguish between these possibilities.

In addition to clarifying the role of Drp1 in the triggering of insulin secretion, our study is the first to identify a link between Drp1 and the amplifying pathway of insulin secretion. While the exact molecular mediator of the amplifying pathway that is deficient remains to be identified, a number of amplifying factors could feasibly be altered by loss of beta cell Drp1. Two attractive possibilities are either disruption of the isocitrate-to-SENP1 pathway, whereby glucose induces an elevation in cytosolic NADPH levels that activate the protease SENP1 and in turn the exocytotic machinery[31], or impaired mitochondrial GTP production[32]. Indeed, our 2-photon imaging revealed decreased NAD(P)H fluorescence in Drp1β-KO islets at 10mM glucose (Figure 2.5 L). However, our unchanged bioluminescence-based measurement of total cellular NADPH suggests that any alterations of the isocitrate-to-SENP1 pathway caused by Drp1 loss are not due to a complete block in glucose-induced NADPH production. Further defining the effect of Drp1 loss on beta-cell metabolism will be an important future direction of our work.

There are several important differences between our data and previous studies examining beta cell Drp1 knockdown *in vitro*. Past studies using Drp1 knockdown or dominant negative Drp1 over-expression in beta cell lines or mDivi-1 mediated Drp1 inhibition in primary mouse islets have reported decreased ATP-linked respiration[7,8] and/or increased proton leak[7,8], in contrast to our findings of normal oxygen consumption in Drp1β-KO islets. This discrepancy could reflect a difference between proliferative beta cell lines and quiescent adult mouse islets[33], a difference in

the consequences of acute *in vitro* vs chronic *in vivo* Drp1 loss, or the recently identified off-target effect of mDivi-1 on ETC Complex I[15]. Furthermore, a previous study[7] suggested that impaired GSIS in mDivi-1 treated islets was caused by decreased substrate availability because it could be rescued by methyl pyruvate treatment. However, we note that methyl pyruvate may directly close K_{ATP} channels instead of acting as a mitochondrial substrate[34], making this rescue difficult to interpret. Our observations of unchanged Drp1β-KO islet respiration (Figure 2.6 A) indicate that even if such an effect on substrate availability exists, it is not sufficient to alter islet respiration and subsequent ATP production at least in the setting of chronic Drp1 loss. Further studies are needed to investigate the *in vitro* versus *in vivo* and acute versus chronic differences observed herein.

Finally, it is noteworthy that Drp1β-Het mice did not exhibit a glucose tolerance phenotype under either normal (Figure 2.1) or HFD conditions (Figure 2.4), despite ~50% reduced Drp1 levels. With the exception of several studies in cardiomyocytes[35,36], Drp1 heterozygosity has not been found to produce a phenotype in most cell types[37]. Our findings further illustrate the highly cell-type specific requirements for mitochondrial dynamics[38].

In summary, our findings establish an important role for beta cell Drp1 in regulating the second phase of GSIS, islet Ca^{2+} handling, and metabolic amplification, and suggest that a greater understanding of the role of mitochondrial fission in beta cells may lead to novel approaches to correct islet dysfunction in diabetes.

2.6 ACKNOWLEDGEMENTS

TGH, MJM, and GMK conceptualized the experiments; TGH, ERC, HRV, DGC, and GMK performed the experiments and analyzed data; TGH and GMK wrote the manuscript; TGH, HS, MJM, and GMK edited the manuscript. GMK is the guarantor of this work and, as such, had full access to all the data in the study and takes responsibility for the integrity of the data and the accuracy of the data analysis. This study was presented at the ADA's 77th and 78th Scientific

Sessions. We would like to thank Michael S. German and Gerold M. Grodsky for helpful discussions, and Vi Dang, Vinh Nguyen and Gregory Szot of the UCSF Islet Production Core for providing pancreatic islets.

This work was supported by NIH/NIDDK (R01 DK107650, and P30 DK087945 - a Pilot and Feasibility Grant to GK and core laboratories). GMK is supported by a Career Development Award from JDRF (5-CDA-2014-199-A-N). ERD is supported by a fellowship from NIH/NIGMS (T32 GM008349). HRV is supported by a postdoctoral fellowship from the American Diabetes Association (1-17-PDF-155). The Merrins lab is additionally supported by grants to MJM from the NIH/NIDDK (R01 DK113103), the NIH/NIA (R21 AG050135), and the American Diabetes Association (1-16-IBS-212) to MJM. The UCSF Islet Isolation Facility is supported by Diabetes Research Center (DRC) grant NIH P30 DK063720.

2.8 FIGURES

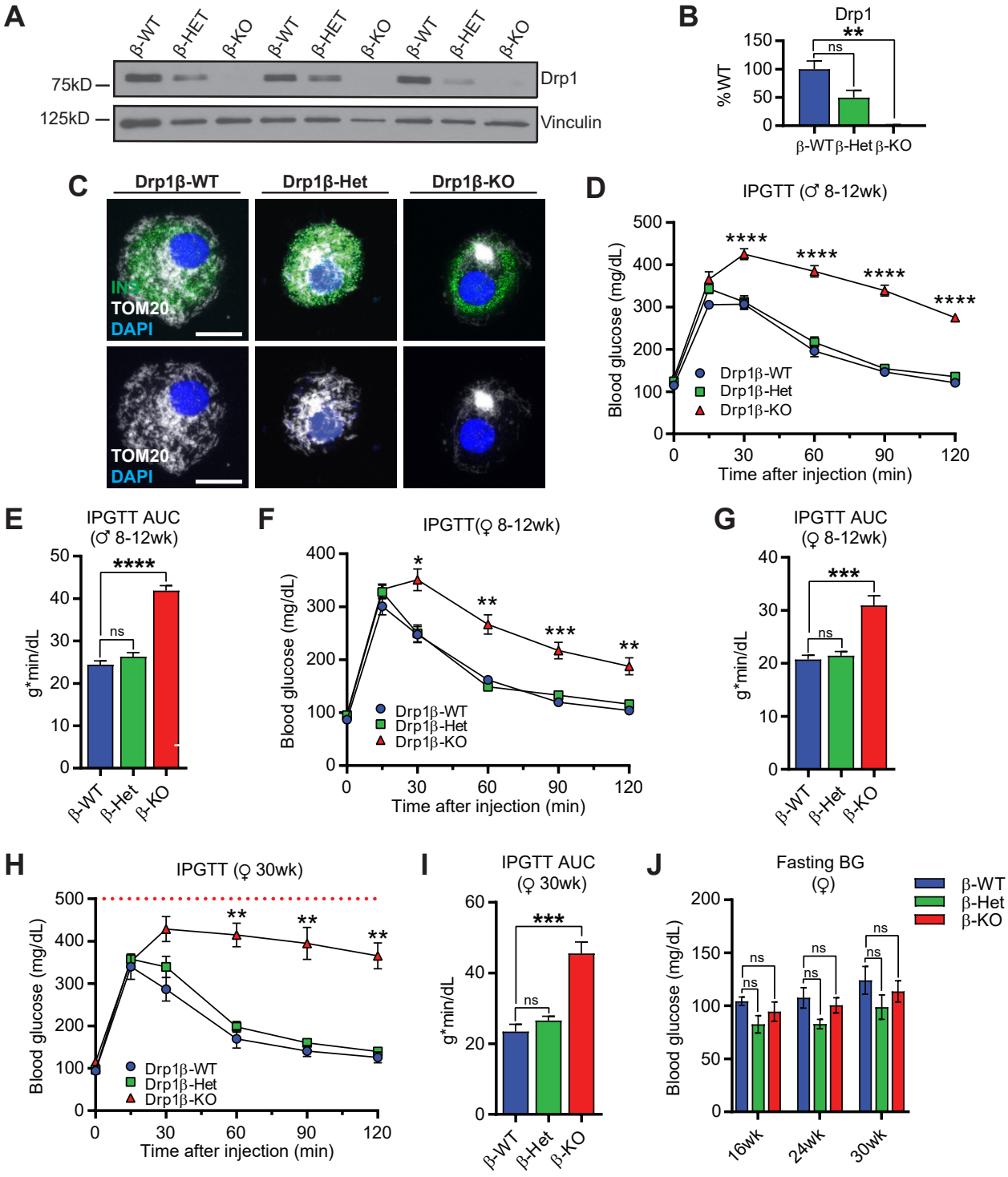

Figure 2.1 Drp1β-KO mice are glucose intolerant.

(A) Western blot for Drp1 and vinculin (loading control) in male 17-18wk old Drp1β-WT, -Het and -KO islets. **(B)** Drp1 signal from (A) quantified and normalized to vinculin and -WT islets. One-way ANOVA: $F(2, 6) = 19.91$, $P=0.0022$. **(C)** Immunofluorescence images of dispersed 13-22wk old islets stained for insulin (green), Tom20 (white) and Dapi (blue). Scale bar is 10μm. **(D)** Intraperitoneal glucose tolerance tests (IPGTT) in male 8-12wk old Drp1β-WT (blue circles) -Het (green squares) and -KO (red triangles) mice. n=8-12 per genotype. Two-way ANOVA with repeated measures: interaction $F(10, 135) = 21.95$, $P<0.0001$; time $F(5, 135) = 266.2$, $P<0.0001$; genotype $F(2, 27) = 72.34$, $P<0.0001$ (Drp1β-WT vs Drp1β-Het, $p = 0.1939$; Drp1β-WT vs Drp1β-KO, $p < 0.0001$). **(E)** AUC analysis of (D). One-way ANOVA: $F(2, 27) = 87.65$, $P<0.0001$. **(F)** Intraperitoneal glucose tolerance tests in female 8-12wk old Drp1β-WT, -Het, and -KO mice. n=8-11 per genotype. Two-way ANOVA with repeated measures: interaction $F(10, 125) = 10.92$, $P<0.0001$; time $F(5, 125) = 331.3$, $P<0.0001$; genotype $F(2, 25) = 16$, $P<0.0001$ (Drp1β-WT vs Drp1β-Het, $p = 0.5881$; Drp1β-WT vs Drp1β-KO, $p < 0.0001$). **(G)** AUC analysis of (F). One-way ANOVA: $F(2, 25) = 18.89$, $P<0.0001$. **(H)** Intraperitoneal glucose tolerance tests in female 30wk old Drp1β-WT, -Het, and -KO mice. n=5 per genotype. Red dotted line represents maximum measurement of 500mg/dL. Two-way ANOVA with repeated measures: interaction $F(10, 60) = 23.44$, $P<0.0001$; time $F(5, 60) = 149$, $P<0.0001$; genotype $F(2, 12) = 23.72$, $P<0.0001$ (Drp1β-WT vs Drp1β-Het, $p = 0.3684$; Drp1β-WT vs Drp1β-KO, $p < 0.0001$). **(I)** AUC analysis of (H). One-way ANOVA: $F(2, 12) = 26.94$, $P<0.0001$. **(J)** Fasting blood glucose values in 16wk, 24wk, and 30wk old female mice. n=4-5 per genotype. Two-way ANOVA: interaction $F(4, 35) = 0.02826$, $P=0.9984$; age $F(2, 35) = 3.504$, $P=0.0410$; genotype $F(2, 35) = 5.383$; $P=0.0092$ (Drp1β-WT vs Drp1β-Het, $p = 0.0051$; Drp1β-WT vs Drp1β-KO, $p = 0.2413$). For all panels significance levels are represented as follows: p-value≤0.05, *; p-value≤0.01, **; p-value≤0.001, ***; p-value≤0.0001, ****.

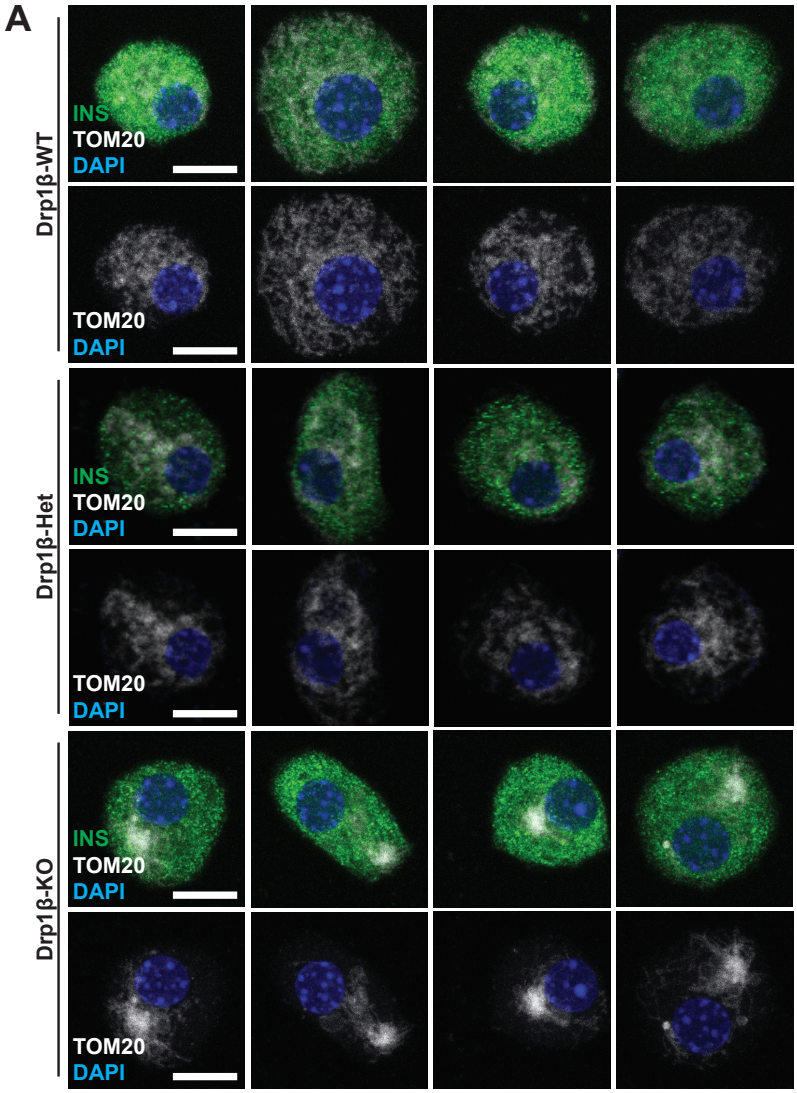

Figure 2.2 Additional images of Drp1β-WT, -Het, and -KO beta cell mitochondrial morphology.

(A) Immunofluorescence images of dispersed male 13-21wk old islets stained for insulin (green), Tom20 (white) and Dapi (blue). Scale bar is 10μm.

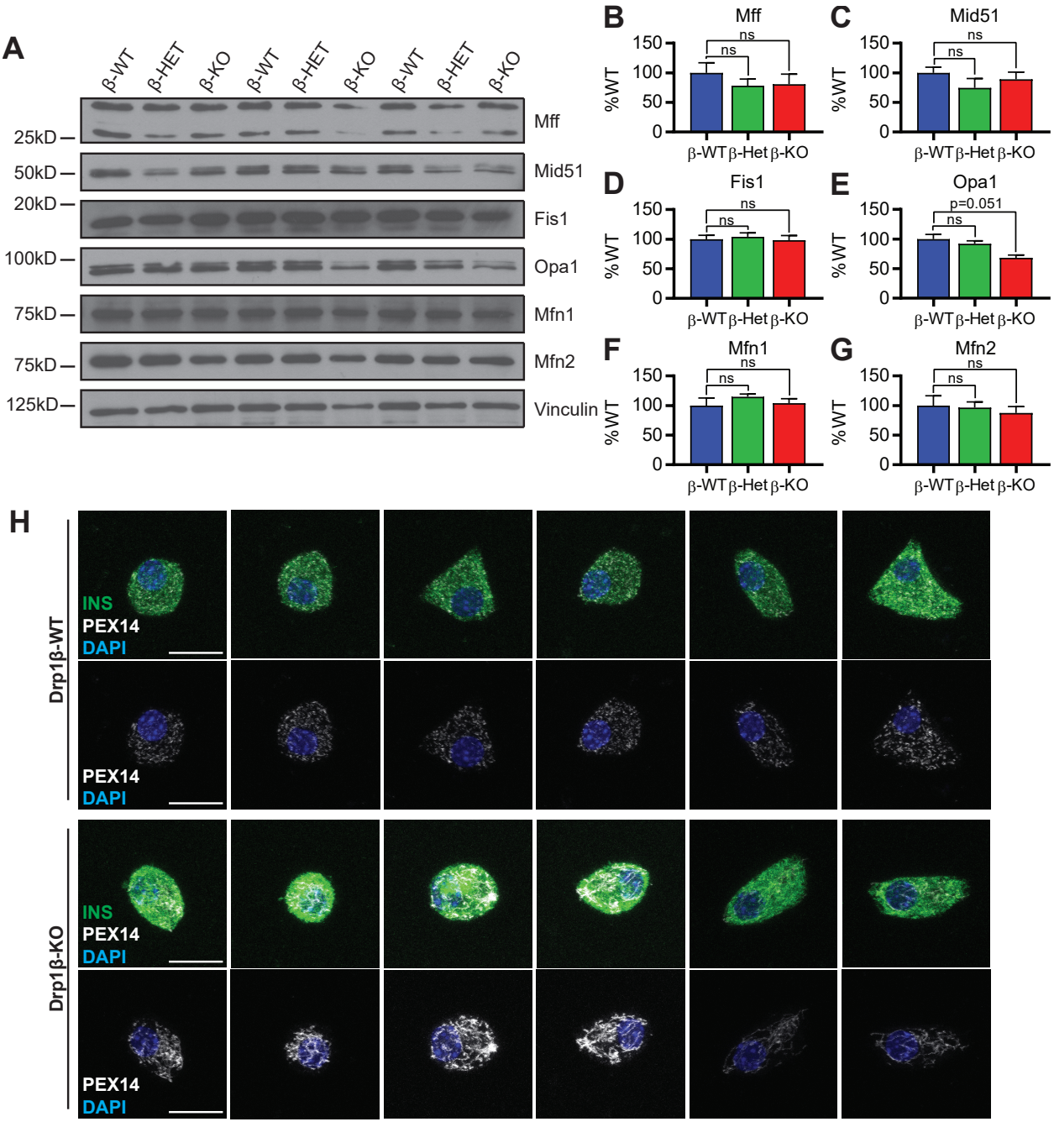

Figure 2.3 Effect of beta cell Drp1 deletion on islet expression of mitochondrial dynamics genes and beta cell peroxisomal morphology.

(A) Western blots of selected mitochondrial dynamics proteins and vinculin in male 17-18wk old Drp1β-WT, -Het, and -KO islets, quantified and normalized to vinculin and average of -WT bands in (B-G). **(B)** Mff. One-way ANOVA: F(2, 6) = 0.5944, P=0.5814. **(C)** MiD51. One-way ANOVA: F(2, 6) = 1.003, P=0.4210. **(D)** Fis1. One-way ANOVA: F(2, 6) = 0.1632, P=0.8530. **(E)** Opa1. One-way ANOVA: F(2, 6) = 7.497, P=0.0233. **(F)** Mfn1. One-way ANOVA: F(2, 6) = 0.7144,

P=0.5269. **(G)** Mfn2. One-way ANOVA: F(2, 6) = 0.2568, P=0.7816. **(H)** Immunofluorescence images of dispersed male 13-21wk old islets stained for insulin (green), Pex14 (white) and Dapi (blue). Scale bar is 10μm. For all panels, significance levels are represented as follows: p-value≤0.05, *; p-value≤0.01, **; p-value≤0.001, ***; p-value≤0.0001, ****.

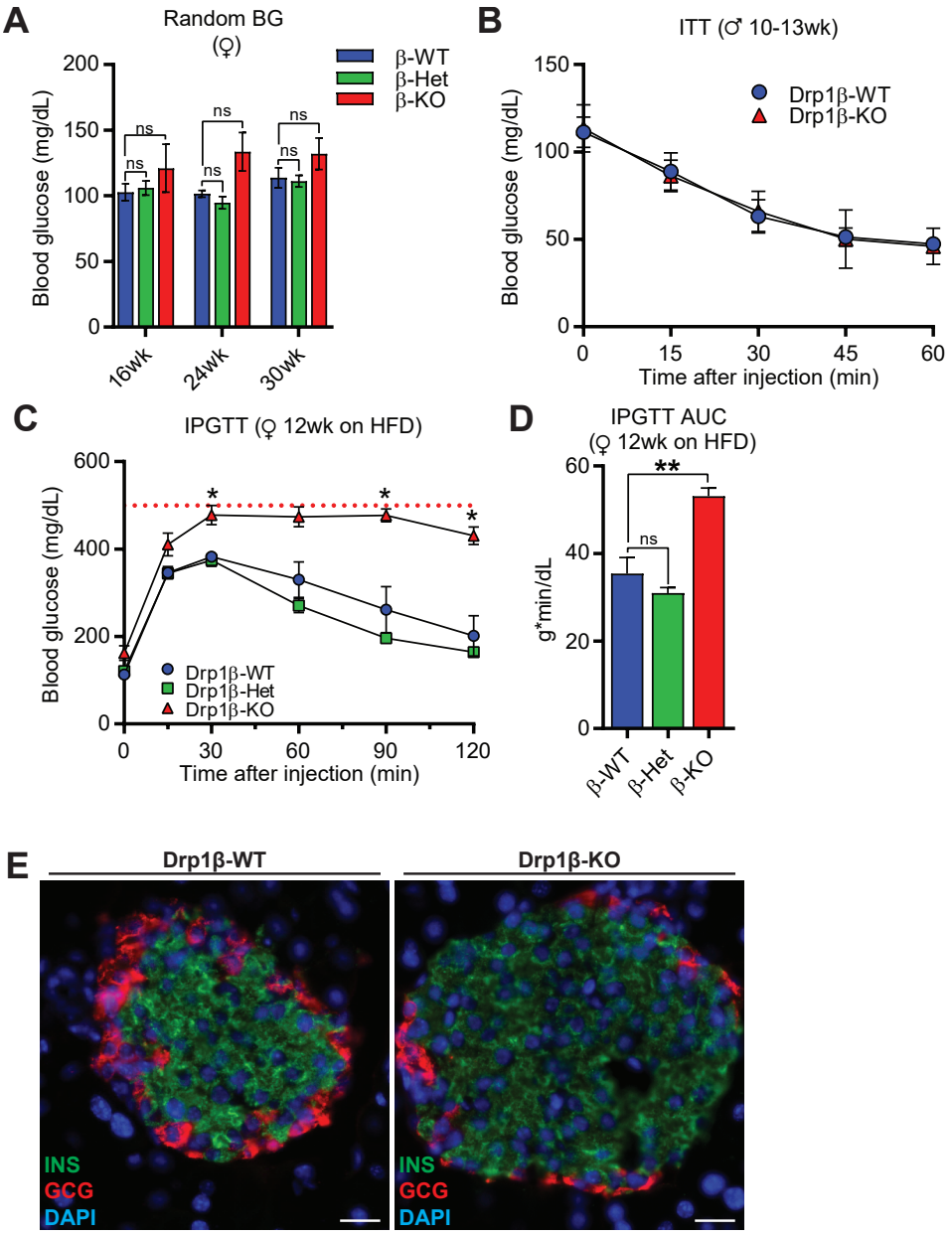

Figure 2.4 Additional metabolic measurements in Drp1β-KO mice.

(A) Random blood glucose values in female Drp1β-WT (blue circles) -Het (green squares) and -KO (red triangles) mice at 16, 24, and 30 weeks of age. n=4-5 mice of each genotype. Two-way ANOVA: interaction $F(4, 35) = 0.4094$, $P=0.8006$; age $F(2, 35) = 0.9003$, $P=0.4157$; genotype $F(2, 35) = 6.012$, $P=0.0057$ (Drp1β-WT vs Drp1β-Het, $p = 0.7909$; Drp1β-WT vs Drp1β-KO, $p = 0.0145$). **(B)** Insulin tolerance test in male Drp1β-WT and -KO mice. n=5-6 mice of each genotype. Two-way ANOVA with repeated measures: interaction $F(4, 36) = 0.2621$, $P=0.9003$; time $F(4, 36) = 148.8$, $P<0.0001$; genotype $F(1, 9) = 0$, $P>0.9999$. **(C)** Intraperitoneal glucose tolerance tests in female Drp1β-WT, -Het, and -KO mice after 12 weeks of high fat diet (HFD). n=6-12 of each genotype. Two-way ANOVA with repeated measures: interaction $F(10, 105) = 11.63$, $P<0.0001$; time $F(5, 105) = 113.3$, $P<0.0001$; genotype $F(2, 21) = 31.41$, $P<0.0001$ (Drp1β-WT vs Drp1β-

Het, p = 0.1997; Drp1β-WT vs Drp1β-KO, p < 0.0001). **(D)** AUC analysis of (B). One-way ANOVA: F(2, 21) = 29.58, P<0.0001. **(E)** Immunofluorescence images of male 9-10wk old pancreata stained for glucagon (red), insulin (green) and Dapi (blue). Scale bar is 20μm. For all panels, significance levels are represented as follows: p-value≤0.05, *; p-value≤0.01, **; p-value≤0.001, ***; p-value≤0.0001, ****.

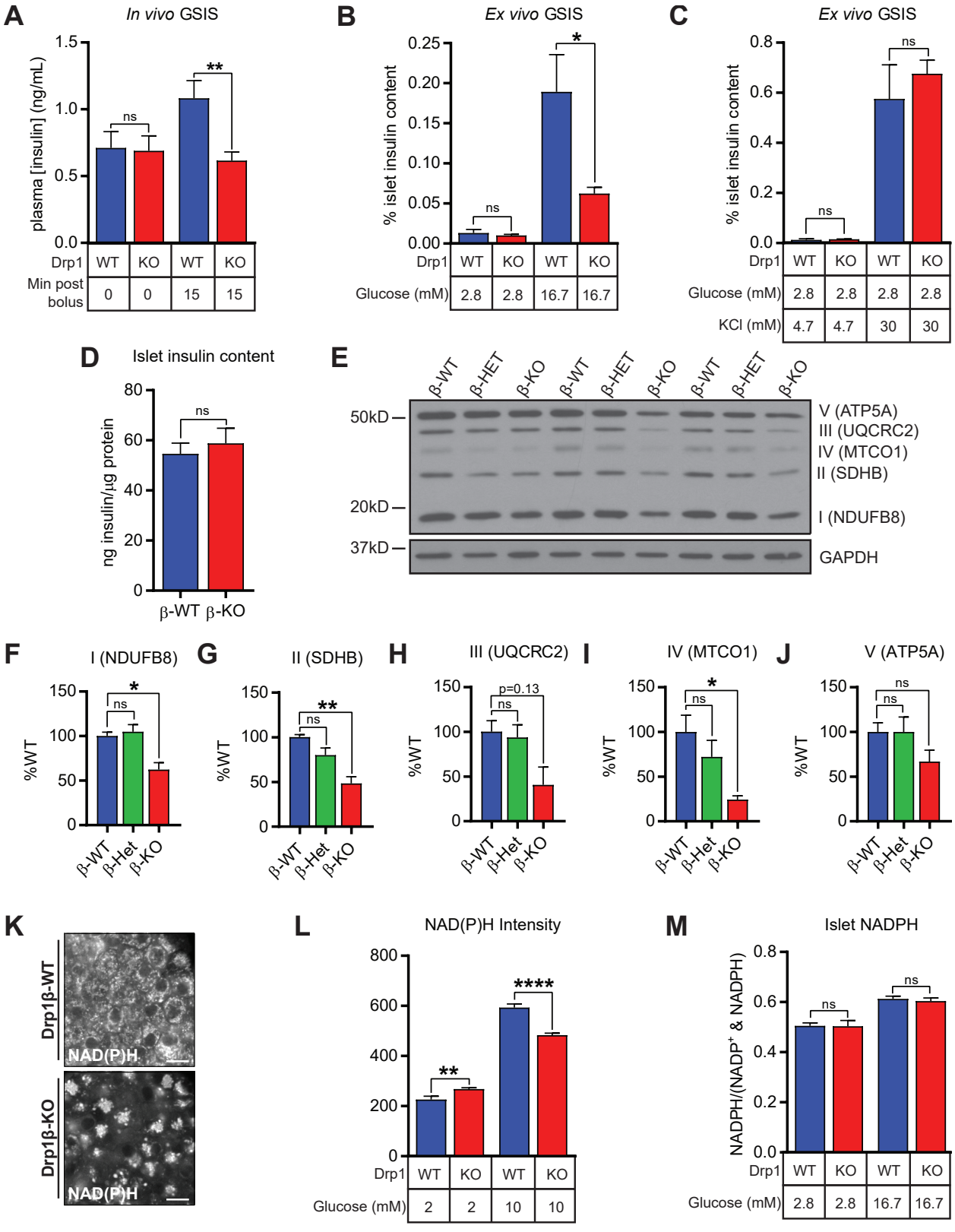

Figure 2.5 Drp1β-KO mice have impaired GSIS and mitochondrial abnormalities.

(A) Plasma insulin measurements in 10wk old male Drp1β-WT and -KO mice. n=17-18 per genotype. Two-way ANOVA with repeated measures: interaction $F(1, 33) = 25.14$, $P<0.0001$; time $F(1, 33) = 11.31$, $P=0.0020$; genotype $F(1, 33) = 2.697$, $P=0.1100$. **(B)** *Ex vivo* GSIS of male 8-17wk old Drp1β-WT and -KO islets in response to 2.8mM and 16.7mM glucose. n=10 per genotype. Two-way ANOVA with repeated measures: interaction $F(1, 18) = 8.214$, $P = 0.0103$; treatment $F(1, 18) = 27.89$, $P<0.0001$; genotype $F(1, 18) = 6.429$, $P = 0.0207$. **(C)** *Ex vivo* GSIS of male 8-12wk old Drp1β-WT and -KO islets in response to 2.8mM glucose and 30mM KCl. n=4-5 per genotype. Two-way ANOVA with repeated measures: interaction $F(1, 7) = 0.5459$, $P=0.4840$; treatment $F(1, 7) = 83.24$, $P<0.0001$; genotype $F(1, 7) = 0.5852$, $P=0.4693$. **(D)** Insulin content from male 7-12wk old male islets. n=9-10 per genotype. Unpaired t-test: P value = 0.5877. **(E)** Western blots of selected ETC complex proteins and GAPDH in 17-18wk old male islets, quantified and normalized to GAPDH and average of -WT bands in (F-J). **(F)** NDUFB8. One-way ANOVA: $F(2, 6) = 11.26$, $P=0.0093$. **(G)** SDHB. One-way ANOVA: $F(2, 6) = 15.93$, $P=0.0040$. **(H)** UQCRC2. One-way ANOVA: $F(2, 6) = 4.252$, $P=0.0708$. **(I)** MTCO1. One-way ANOVA: $F(2, 6) = 6.322$, $P=0.0333$. **(J)** ATP5A. One-way ANOVA: $F(2, 6) = 2.045$, $P=0.2103$. **(K)** Two-photon NAD(P)H images from Drp1β-WT and -KO islets. **(L)** Quantified NAD(P)H intensity in 6-7wk old male islets. n=48-54 islets from 5 mice of each genotype. Two-way ANOVA: interaction $F(1, 143) = 57.27$, $P<0.0001$; treatment $F(1, 143) = 842.1$, $P<0.0001$; genotype $F(1, 143) = 11.71$, $P=0.0008$. **(M)** Islet NADPH levels in dispersed 12-22wk old male Drp1β-WT and -KO islets 15min after exposure to 2.8mM or 16.7mM glucose. n=9 replicates from 3 mice of each genotype. Two-way ANOVA: interaction $F(1, 16) = 0.1408$, $P=0.7125$; treatment $F(1, 16) = 111.6$, $P<0.0001$; genotype $F(1, 16) = 0.081$, $P=0.7796$. For all panels, post-hoc significance levels are represented as follows: p-value≤0.05, *; p-value≤0.01, **; p-value≤0.001, ***; p-value≤0.0001, ****.

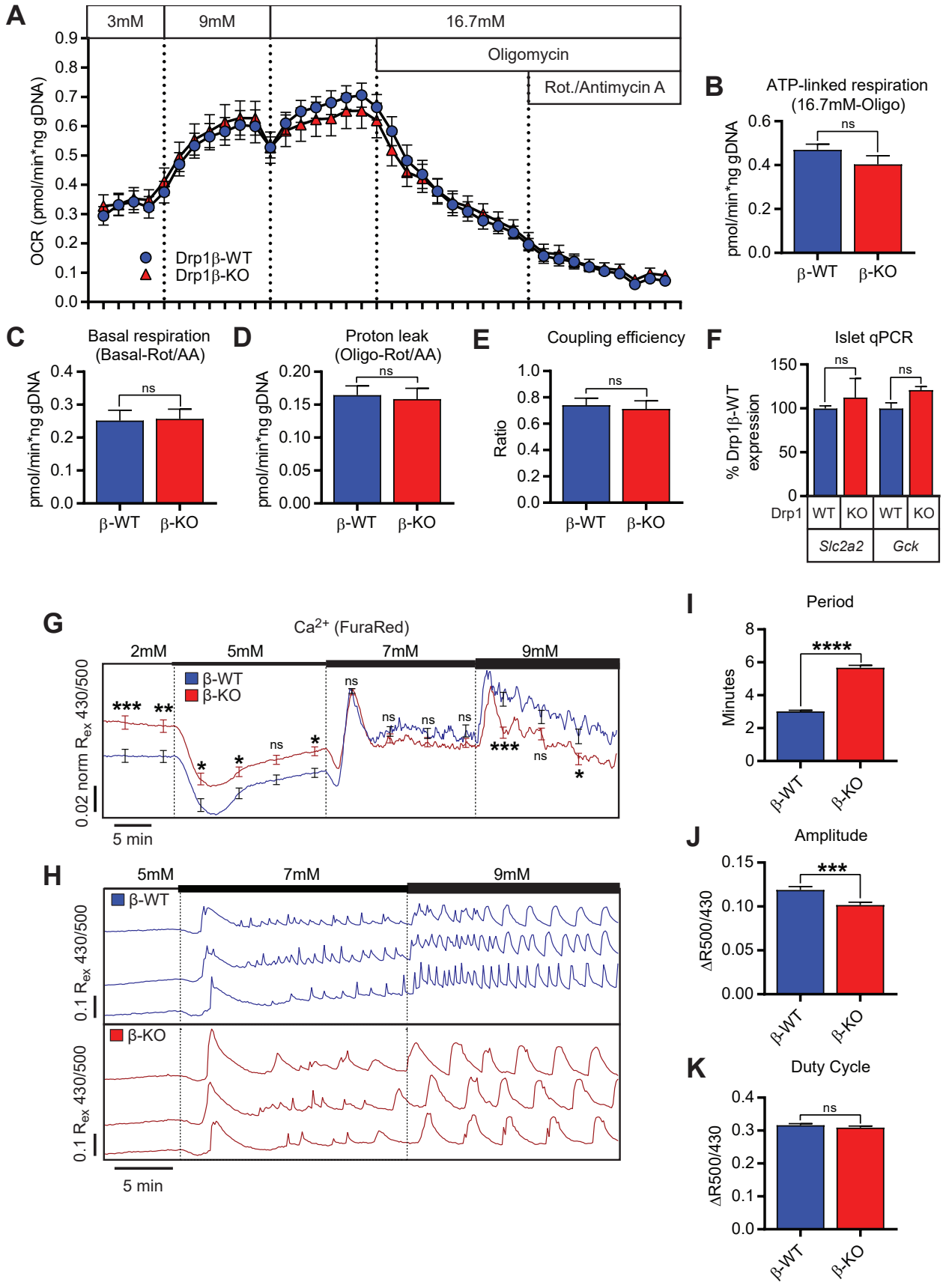
A
3mM
9mM
16.7mM
Oligomycin
Rot./Antimycin A
OCR (pmol/min*ng gDNA)
Drp1β-WT
Drp1β-KO
B
ATP-linked respiration
(16.7mM-Oligo)
pmol/min*ng gDNA
ns
β-WT
β-KO
C
Basal respiration
(Basal-Rot/AA)
D
Proton leak
(Oligo-Rot/AA)
E
Coupling efficiency
Ratio
F
Islet qPCR
% Drp1β-WT expression
Drp1
WT
KO
Slc2a2
Gck
G
Ca2+ (FuraRed)
2mM
5mM
7mM
9mM
β-WT
β-KO
0.02 norm Rex 430/500
5 min
H
0.1 Rex 430/500
I
Period
Minutes
****
J
Amplitude
ΔR500/430
***
K
Duty Cycle

Figure 2.6 Beta cell Drp1 deletion does not affect islet oxygen consumption or the glucose threshold for Ca^{2+} entry.

(A) Oxygen consumption rates (OCR) in islets from 8-11wk old male Drp1β-WT (blue circles) and -KO (red triangles) mice. n=12-18 from 4 mice of each genotype. Two-way ANOVA with repeated measures: interaction F(37, 1036) = 0.8141, P=0.7785; time F(37, 1036) = 163.9, P<0.0001; genotype F(1, 28) = 0.0002147, P=0.9884. **(B-E)** Respiration parameters calculated from OCRs in (A). **(B)** ATP-linked respiration. Unpaired t-test: P value = 0.2223. **(C)** Basal respiration. Unpaired t-test: P value = 0.8950. **(D)** Proton leak. Unpaired t-test: P value = 0.7929. **(E)** Coupling efficiency. Unpaired t-test: P value = 0.2015. **(F)** qPCR measurement of islet Glut2 (*Slc2a2*) and *Gck* expression in 11-16wk old Drp1β-WT and -KO islets. n=3-4 mice of each genotype. Unpaired t-test, Slc2a2: P value >0.99, Gck: P value = 0.1042. **(G)** Average cytosolic Ca^{2+} in male 11-17wk old islets in response to escalating glucose concentrations, normalized to 5mM KCN treatment. n=115-131 islets from 6 mice of each genotype. Two-way ANOVA: interaction F(13, 3416) = 8.437, P<0.0001; time F(13, 3416) = 43.9, P<0.0001; genotype F(1, 3416) = 0.7382, P=0.3903. Asterisks represent results of Holm-Sidak corrected unpaired t-tests. **(H)** Example islet Ca^{2+} oscillations in 5mM, 7mM and 9mM glucose. **(I)** Period calculations from islet Ca^{2+} traces in 9mM glucose. n=152-154 islets from 6 mice of each genotype. Unpaired t-test: P value <0.0001. **(J)** Amplitude calculation from islet Ca^{2+} traces in 9mM glucose. n=152-154 islets from 6 mice of each genotype. Unpaired t-test: P value = 0.0005. **(K)** Duty cycle calculation from islet Ca^{2+} traces in 9mM glucose. Unpaired t-test: P value = 0.2533. n=152-154 islets from 6 mice of each genotype. For all panels, significance levels are represented as follows: p-value≤0.05, *; p-value≤0.01, **; p-value≤0.001, ***; p-value≤0.0001, ****.

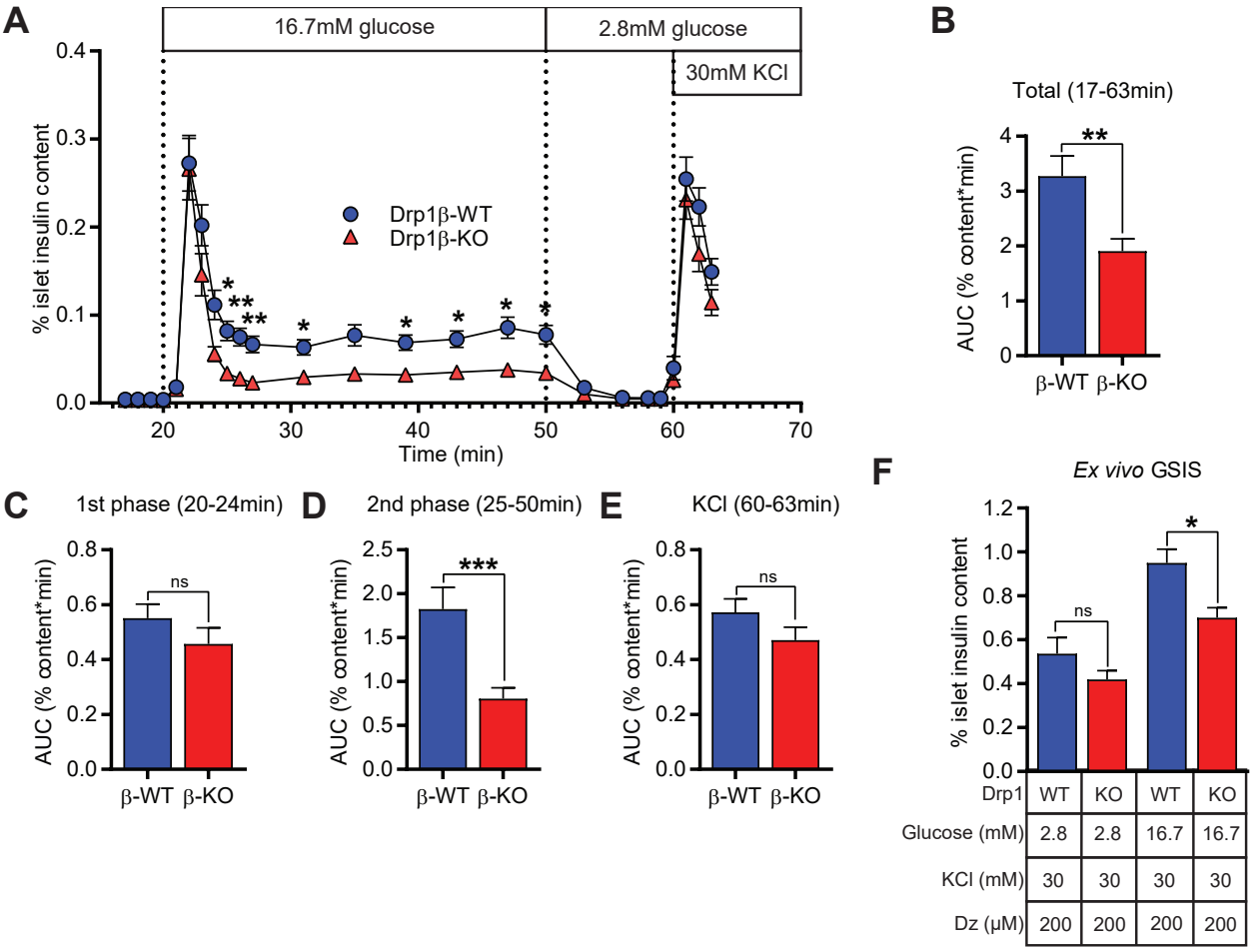

Figure 2.7 Loss of beta cell Drp1 impairs 2nd phase insulin secretion and the metabolic amplifying pathway.

(A) Dynamic insulin secretion in female 7-12wk old Drp1β-WT and -KO islets. n=16 from 8 mice of each genotype. Two-way ANOVA with repeated measures: interaction F(24, 720) = 2.151, P=0.0012; time F(24, 720) = 107.8, P<0.0001; genotype F(1, 30) = 6.709, P=0.0147. **(B-E)** AUC analyses of (A). **(B)** Total AUC. Unpaired t-test: P value = 0.0035. **(C)** 1st phase AUC, representing secretion from minutes 20-24. Unpaired t-test: P value = 0.2380. **(D)** 2nd phase AUC, representing minutes 25-50. Unpaired t-test: P value = 0.0009. **(E)** KCl AUC, representing secretion minutes 60-63. Unpaired t-test: P value = 0.1461. **(F)** *In vitro* GSIS of male 7-9wk old Drp1β-WT and -KO islets in response to 2.8mM or 16.7mM glucose in the presence of both 200mM diazoxide and 30mM KCl. n=6 of each genotype. Two-way ANOVA with repeated measures: interaction F(1, 10) = 1.736, P=0.2170; treatment F(1, 10) = 47.81, P<0.0001; genotype F(1, 10) = 8.537, P=0.0153. For all panels, significance levels are represented as follows: p-value≤0.05, *; p-value≤0.01, **; p-value≤0.001, ***; p-value≤0.0001, ****.

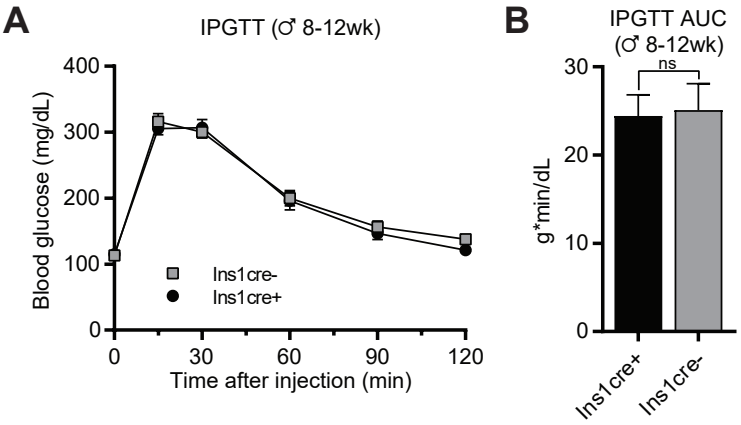

Figure 2.8 Glucose tolerance in Drp1β-WT mice is not affected by the presence of the Ins1^{cre} allele

(A) Intraperitoneal glucose tolerance test (IPGTT) in male Drp1β-WT mice harboring one *Ins1^{cre}* allele (*Ins1$^{cre/+}$; Drp1$^{+/+}$*, black circles) or zero Ins1-cre alleles (*Ins1$^{+/+}$;* any Drp1 genotype, grey squares). n=8-13. Two-way ANOVA with repeated measures: interaction F(5, 95) = 0.4987, P=0.7765; time F(5, 95) = 206.2, P<0.0001; genotype F(1, 19) = 0.3589, P=0.5562. **(B)** AUC calculations from (A). Unpaired t-test: P value = 0.5986. For all panels, significance levels are represented as follows: p-value≤0.05, *; p-value≤0.01, **; p-value≤0.001, ***; p-value≤0.0001, ****.

CHAPTER 3: Materials and Methods

Content in this chapter was modified from the following publication:

Hennings TG, Chopra DG, DeLeon ER, VanDeusen HR, Sesaki H, Merrins MJ, Ku GM. In Vivo Deletion of β-Cell Drp1 Impairs Insulin Secretion Without Affecting Islet Oxygen Consumption. Endocrinology. 2018 Sep 1;159(9):3245-3256. doi: 10.1210/en.2018-00445.

3.1 Animals

Dnm1l$^{tm1.1hise}$ (MGI 4366510) and *Ins1*$^{tm1.1(cre)Thor}$ (MGI 5614359) alleles have been described previously[16,17] and are hereafter referred to as *Drp1*^{f} and *Ins1*^{cre}, respectively. Mice were maintained on a C57Bl/6 background. All mice were verified to be homozygous for the C57Bl/6J allele of the nicotinamide nucleotide transferase (*Nnt*)[39]. The following abbreviations were used for mouse genotypes: Drp1β-KO (*Ins1*$^{cre/+}$*;Drp1*$^{f/f}$), Drp1β-Het (*Ins1*$^{cre/+}$*;Drp1*$^{f/+}$), Drp1β-WT (*Ins1*$^{cre/+}$*;Drp1*$^{+/+}$, *Ins1*$^{+/+}$*;Drp1*$^{+/+}$, *Ins1*$^{+/+}$*;Drp1*$^{f/+}$, *Ins1*$^{+/+}$*;Drp1*$^{f/f}$). Drp1β-WT mice included *Ins1*$^{+/+}$ mice of any Drp1 genotype since the presence of a single copy of the *Ins1*^{cre} allele was not found to affect glucose tolerance on a chow diet (Figure 2.8). Mice were group-housed in a colony maintained with a standard 12h light/dark cycle and given food and water ad libitum. Experiments were conducted according to the Guide for the Care and Use of Laboratory Animals, as adopted by the National Institutes of Health, and with approval of the UCSF Institutional Animal Care and Use Committee. For intraperitoneal glucose tolerance tests, mice were individually housed and fasted for 6 hours before injection of glucose (2mg/g body mass), after which tail vein blood glucose measurements were made at regular intervals. Plasma insulin samples were collected prior to and 15min after intraperitoneal glucose injection and analyzed by ELISA (Mercodia 10-1247-10). For high fat diet (HFD) experiments, 10wk old female mice were fed Envigo TD.07011 (4.9 Kcal/g, 21% from protein, 24.6% from carbohydrates, and 54.4% from fat) for 12 weeks. For all other experiments, animals were fed PicoLab Mouse Diet 20 (3.75 Kcal/g, 23.2% from protein, 55.2% from carbohydrates, 21.6% from fat). Pancreatic islets isolations were conducted according to a previously described protocol[40].

3.2 Immunofluorescence Imaging

For imaging of mitochondrial morphology in individual beta cells, islets were first rested overnight in islet media (RPMI with 10% fetal bovine serum, 1% penicillin/streptomycin, 25mM

HEPES), then dissociated with 0.25% trypsin and plated onto glass coverslips coated with 804G cell conditioned media. Two days after plating, cells were fixed in 4% paraformaldehyde for 10min at 37°C, permeabilized in 0.1% Triton X-100 in PBS for 1 hour at room temperature (RT), blocked in 10% donkey serum for 1 hour at RT, and incubated in primary antibody overnight at 4°C in 1% donkey serum. Secondary antibodies were incubated for 1 hour at RT. Z-stacks were collected by confocal microscope at 63x (Leica SP5) for images of mitochondrial morphology using Tom20 immunostaining in order to accurately represent the three-dimensional nature of mitochondria. For peroxisomal morphology, cells were fixed as above but were permeabilized in 0.5% Triton X-100 in PBS for 15min at RT, blocked in 2% BSA in PBS for 1 hour at RT, and incubated in primary antibody overnight in 2% BSA at 4°C. Primary antibodies used: rabbit anti-Tom20 (1:500, Santa Cruz sc11415; RRID:AB_2207533); rabbit anti-Pex14 (1:200, ProteinTech 10594-1-AP, RRID:AB_2252194) guinea pig anti-insulin (1:500, Dako A0564, RRID:AB_10013624).

For immunohistochemistry, pancreata were fixed in 4% PFA and frozen in optimal cutting temperature compound (OCT). 6µm sections were permeabilized in 0.1% Triton X-100 and stained. Primary antibodies used: guinea-pig anti-insulin (1:250, Dako A0564, RRID:AB_10013624), rabbit anti-glucagon (1:250, Dako A0565, RRID:AB_10013726). Secondary antibodies: anti-guinea pig Alexa Fluor 488 (1:500, Life Technologies A11073, RRID:AB_142018), anti-rabbit Alexa Fluor 555 (1:500, Life Technologies A31572, RRID:AB_162543), goat anti-guinea pig Alexa 647 (1:500, Life Technologies A21450, RRID:AB_141882).

3.3 Western Blots

Protein was extracted from pancreatic islets using radioimmune precipitation (RIPA) buffer containing complete protease inhibitors (Roche). Lysates were sonicated on ice for 5 minutes with alternating 30 second pulses and rests, and pre-cleared by centrifugation at 15,000xg for 5min at

4°C. Bio-Rad Mini-Protean Tetra and Trans-Blot Turbo systems were used for PAGE gel electrophoresis and PVDF membrane transfer, respectively. Band intensities were quantified using ImageJ software[41]. Primary antibodies used were mouse anti-DLP1 (1:1000, BD 61113, RRID:AB_398424), mouse anti-GAPDH-peroxidase (1:20000, Sigma G9295, RRID:AB_1078992), mouse anti-rodent OXPHOS (1:1000, Abcam ab110413, RRID:AB_2629281), rabbit anti-vinculin (1:1000, Cell Signaling 13901, RRID:AB_2728768), rabbit anti-Fis1 (1:1000, Proteintech 10956-1-AP, RRID:AB_2102532), rabbit anti-Mff (1:1000, Proteintech 17090-1-AP, RRID:AB_2142463), rabbit anti-Mid51 (1:500, Proteintech 20164-1-AP, RRID:AB_10639522), rabbit anti-Mfn1 (1:1000, Proteintech 13798-1-AP, RRID:AB_2266318), rabbit anti-Mfn2 (1:1000, Proteintech 12186-1-AP, RRID:AB_2266320), and rabbit anti-Opa1 (1:1000, Cell Signaling 80471, RRID:AB_2734117). Secondary antibodies used were horse anti-mouse HRP (1:10000, Cell Signaling 7076, RRID:AB_330924) and goat anti-rabbit HRP (1:10000, Cell Signaling 7074, RRID:AB_2099233).

3.4 Glucose-Stimulated Insulin Secretion (GSIS)

Islets were rested for 24 hours after isolation in islet media (RPMI with 10% fetal bovine serum, 1% penicillin/streptomycin, 25mM HEPES). For static GSIS, 20 islets were hand-picked and equilibrated in Krebs-Ringer Bicarbonate HEPES buffer (KRBH; 137mM NaCl, 4.7mM KCl, 1.2mM KH_2PO_4, 1.2mM $MgSO_4$, 2.5mM $CaCl_2$, 25mM $NaHCO_3$, 20mM HEPES, 0.25% BSA) containing 2.8mM glucose for 1 hour at 37°C. Equilibration buffer was then removed and islets were sequentially stimulated with KRBH containing concentrations of glucose and compounds as indicated. Islets were lysed in RIPA buffer for determination of total islet insulin content for stimulation buffer insulin measurement normalization. Dynamic GSIS was carried out on a Biorep perifusion system according to manufacturer's protocol.

3.5 Oxygen Consumption Rates

Islet oxygen consumption measurements were conducted on a Seahorse XFe24 machine (Agilent). Islets were placed in the wells of an Islet plate in XF Base Media with 3mM glucose and equilibrated at 37°C for 1hour in a CO_2-free incubator. Drug concentrations: oligomycin A (5μM), rotenone (5μM) antimycin A (5 μM). OCRs were normalized to islet DNA content.

3.6 Two Photon Imaging of NAD(P)H

NAD(P)H images were collected as in Gregg et al[24]. NAD(P)H was excited with Mai Tai DeepSee Ti:Sapphire laser (Spectra-Physics) at 740 nm with a 450/70m bandpass emission filter (Chroma) before being collected by a Hamamatsu H7422P-40 GaAsP photomultiplier tube. Images were collected with a Nikon Plan Apo 60x/1.4NA objective at 256x256 resolution with 120 s (1/s) collection using SPC-830 Photon Counting Electronics (Becker & Hickl GbmH). A single region of interest was used to quantify average islet NAD(P)H fluorescence intensity using Fiji[41].

3.7 Islet $NADP^+$ and NADPH

Islets were rested for 24 hours after isolation in standard islet media (RPMI 1640, 10% FBS, 1% Penicillin/streptomycin, 125mM HEPES). Islets were dispersed, plated, and rested for an additional 24 hours. $NADP^+$ and NADPH were measured using the NADP/NADPH-Glo (Promega G9081) kit following a 15min challenge with either 2.8mM KRBH or 16.7mM KRBH.

2.8 Islet qPCR

Islets were rested for 24 hours after isolation in standard islet media (RPMI 1640, 10% FBS, 1% Penicillin/streptomycin, 125mM HEPES). RNA samples and cDNA libraries were prepared using DirectZol (Zymo) and Superscript III Reverse Transcriptase (Thermo), respectively. qPCR

analysis was carried out using a QuantStudio 5 Real-Time PCR system (Applied Biosystems). *Slc2a2* and *Gck* expression in each islet was calculated using the delta delta Ct method relative to the average of *Ppia* and *Actb*. Primers utilized are as follows: *Slc2a2* (mm00446229_m1); *Gck* (F: GAGATGGATGTGGTGGCAAT, R: TCACATTGGCGGTCTTCATA, probe: GACACGGTGGCCACAAT); *Ppia* (F: GGCCGATGACGAGCCC, R: TGTCTTTGGAACTTTGTCTGCAA, probe: TGGGCCGCGTCTCCTTCGA); *Actb* (F: TTCAACACCCCAGCCATGTA, R: TGTGGTACGACCAGAGGCATAC, probe: TAGCCATCCAGGCTGTGCTGTCCC).

2.9 Timelapse imaging of cytosolic islet Ca^{2+}

Imaging conditions match those described in Gregg et al[24], with an added islet labeling protocol that allowed for simultaneous imaging of Drp1β-WT and Drp1β-KO islets. Islets were labeled for 10 min at 37°C in media containing 1.25 µg/mL diR (Molecular Probes D-12731) prepared from a concentrated stock of 1 mg/mL in DMSO (stored at 4°C), followed by preincubation in 2.5 µM FuraRed AM (Molecular Probes F3020) for 45 min at 37°C. The islets were then transferred to the imaging chamber where a single diR image was taken using a Chroma Cy7 cube (Exciter, ET710/75x; dichroic, T760lpxr, Emitter, ET810/90m). We confirmed that the presence diR had no effect on Ca^{2+} oscillations in wild-type mice. Ca^{2+} was imaged using a Semrock FF444/521/608-Di01 dichroic in combination with Chroma ET430/20x and ET500/20x exciters and an ET630/70m emitter. The FuraRed ratio was reported as the 430/500 excitation ratio normalized to signal in the presence of 5mM KCN. The solution flow rate was maintained at 0.35 mL/min using an MCFS-EZ microfluidic flow control system (Fluigent), and temperature was maintained at 33°C using inline and solution heaters (Warner). Fluorescence emission was collected with a Hamamatsu ORCA-Flash4.0 V2 Digital CMOS camera with a sampling interval of 6 s. A single region of

interest was used to quantify the average response of each islet using Nikon Elements and MathWorks MATLAB software.

2.10 Statistical Analysis

Data are presented as mean ± SEM. Statistical tests were completed using Prism (Graphpad) as described in figure legends. The Holm-Sidak multiple comparisons test was used to make comparisons between group means in two-way ANOVA analyses with three groups. For one- and two-way ANOVA analyses, the results of Bonferroni corrected unpaired t-tests (or other test as indicated in figure legends) were used to make Drp1β-WT versus Drp1β-KO and Drp1β-WT versus Drp1β-Het comparisons at individual time points and are displayed on figure panels.

CHAPTER 4: DISCUSSION

4.1 CONTRIBUTIONS TO THE FIELD

4.1.i First in vivo *disruption of beta cell mitochondrial fission*

This study is the first description of the consequences of *in vivo* disruption of beta cell mitochondrial fission. A number of studies had previously been conducted *in vitro* examining the consequences on insulin secretion of loss or inhibition of beta cell Drp1[6–8]. For all of the reasons listed below, our *in vivo* model of beta cell Drp1 loss represents the most robust description of the consequences of altering beta cell mitochondrial fission that has been reported to date. First, adult beta cells exhibit very low rates of proliferation *in vivo*[42], and the most commonly used murine beta cell lines are highly proliferative. The altered metabolic demands induced by this increased rate of replication[43] can confound the study of the delicate metabolic circuitry required for proper GSIS[44]. Second, beta cells are heterogeneous[45], and this heterogeneity is lost when clonal beta cell lines are used as a substitute for primary islets. Third, beta cells residing within an islet have direct and indirect contact with other cell types that have been shown to influence many aspects of beta cell biology[46]. Finally, mitochondrial metabolism is altered by a myriad of factors that are not completely recapitulated *in vitro* in cell culture conditions[47,48]. Thus, future studies of mitochondrial dynamics in beta cells should rely on *in vivo* systems as much as possible.

4.1.ii Drp1 regulates the amplifying pathway of GSIS

This study places Drp1 among a small number of other factors involved in regulating the contribution of metabolic amplification to GSIS[11,49]. Amplification of insulin secretion, both metabolic and neurohormonal, is widely appreciated as being both crucial to normal physiological insulin secretion as well as a tractable therapeutic target[11,49,50]. Indeed, GLP-1 receptor agonists, a drug class commonly used in type 2 diabetes, exert their beneficial effects on glycemia at least partially by increasing intracellular beta cell cAMP levels.

Future investigations are needed to determine if Drp1, or mitochondrial dynamics more generally, can be targeted for therapeutic benefit. The first step in these efforts should be to more

precisely define how loss of beta cell Drp1 impairs metabolic amplification of insulin secretion. A number of possible mechanisms could feasibly be at play. Given the reductions in ETC complexes and NAD(P)H production that we measured herein (Figure 2.5), the most likely explanation is that Drp1 loss disrupts the TCA cycle in a manner that alters levels of a metabolite involved in metabolic amplification. Candidate metabolites that meet these criteria are malate, citrate, and isocitrate, as all three participate in cataplerotic / anaplerotic cycling with pyruvate to generate cytosolic NADPH[49]. Alternatively, it may be that loss of Drp1 indirectly reduces neurohormonal amplification of insulin secretion by impairing mitochondrial GTP production[32]. GTP is required to translate the pro-secretory signal from Gα(s) coupled G-protein coupled receptors (e.g. the GLP-1 receptor) into increased intracellular cAMP, the main neurohormonal amplifying factor.

Apart from mitochondrial fission, Drp1 has also been described to participate in several extra-mitochondrial processes, including peroxisomal fission[18–20] and plasma membrane vesicle endocytosis[51]. We observed abnormal peroxisomal morphology in beta cells from Drp1β-KO islets (Figure 2.3). Given the central role of mitochondrial metabolism in GSIS, the mitochondria are the most likely location of the insulin secretion defect in the Drp1β-KO mice. Nonetheless, we cannot exclude the contribution peroxisomal defects, endocytosis defects, or alterations in undescribed functions of Drp1 to the impaired GSIS we describe here. Indeed, a number of reports have demonstrated a role for plasma membrane endocytosis in insulin secretion[52]. To determine the contribution of these extra-mitochondrial roles to impaired Drp1β-KO GSIS, we will attempt to correct the unbalanced mitochondrial dynamics by individually co-deleting from the beta cell both Drp1 and the mitochondrial fusion proteins Mfn1 and Mfn2[4], which do not play a role in peroxisomal fission or endocytosis. If these Drp1;Mfn1β-KO and Drp1;Mfn2β-KO mice show an improvement in glucose tolerance and insulin secretion, then the Drp1β-KO phenotype can be confidently ascribed to the mitochondria. A precedence exists for this approach: cardiomyopathy induced by deletion of the mitochondrial fission protein Mff can be rescued by co-deletion of Mfn1 and Mfn2.[53]

4.2 FUTURE DIRECTIONS

4.2.i Characterize the role of other mitochondrial dynamics proteins in beta cell biology

Our work raises the question of whether only Drp1, or also other mitochondrial dynamics proteins are required for proper GSIS. Past experiments had identified requirements for both Opa1, a mitochondrial fusion protein[13], and prohibitin in insulin secretion[14]. Future studies will further investigate the roles of other mitochondrial fission, fusion, and mitophagy proteins in insulin secretion. Additionally, we will seek to determine whether the mitochondrial functions that these proteins govern are mutually exclusive or if they converge on a common machinery, such as with the co-deletion experiment described in the previous section.

4.2.ii Define the role of beta cell Drp1 outside of insulin secretion

In other cell types, Drp1 has been shown to play a role in as diverse cellular processes as apoptosis, intracellular organellar organization, and mitochondrial DNA replication, among others[4,54–57]. It is both feasible and likely that in the beta cell, Drp1 is required for both proper insulin secretion and other cell biological processes relevant to preserving beta cell function and survival in diabetes. Indeed, a number of reports describe a role for Drp1 in beta cell apoptosis *in vitro*[58–62]. Future studies will be necessary to identify the full impact of Drp1 loss and mitochondrial fission more broadly on these additional aspects of beta cell biology *in vivo*.

4.2.iii Further explore the interdependency of mitochondrial fission and function.

There is a clear interdependency between mitochondrial dynamics and mitochondrial function, but the hierarchy of this relationship remains poorly defined[4]. The prevailing model is a bi-directional relationship: alterations in mitochondrial dynamics are sufficient to alter oxidative phosphorylation, and perturbations in oxidative phosphorylation are sufficient to influence mitochondrial morphology. Gaining additional clarity into the nature of this relationship is perhaps

the most promising future direction for the field of mitochondrial dynamics, as targeting mitochondrial dynamics may prove to be more viable route of treating diseases involving defective mitochondrial respiration than targeting mitochondrial respiration directly.

4.2.iv Determine the involvement of altered mitochondrial dynamics in diabetes

It remains to be conclusively determined whether Drp1, or mitochondrial dynamics more generally, are involved in the pathogenesis of diabetes. Several lines of evidence suggest that mitochondrial dynamics are abnormal in type 2 diabetic islets. First, several studies have reported a fragmented mitochondrial morphology present in the beta cells from rodent models of type 2 diabetes[63,64]. Second, expression of Drp1 and several other mitochondrial dynamics protein have been found to be decreased in islets from type 2 diabetic islets[65]. Whether these changes contribute to the impaired GSIS from type 2 diabetic islets or are merely an unrelated consequence of the diabetic milieu will be the focus of additional studies going forward.

Several human diseases either caused by mutations in mitochondrial dynamics proteins or characterized by an imbalance between mitochondrial fission and fusion have inspired the development of pharmaceuticals targeting mitochondrial dynamics. For example, an activator of Mfn2 was recently found to have efficacy in preclinical models of Charcot-Marie-Tooth disease type 2A (CMT2A)[66], a peripheral neuropathy condition in some instances caused by mutations in the mitochondrial fusion protein Mitofusin 2 (Mfn2)[56]. Several inhibitors of Drp1 have been developed[67–69] which have shown efficacy in a number of rodent disease models[56]. However, studies with the most widely used Drp1 inhibitor, mDivi-1, were recently called into question by a report of off-target effects via binding to the electron transport chain complex I[15]. Nonetheless, these compounds could easily be tested in experimental models of diabetes if a role for mitochondrial dynamics in diabetes pathogenesis is discovered.

REFERENCES

1. Ovalle F, Grimes T, Xu G, et al. Verapamil and beta cell function in adults with recent-onset type 1 diabetes. *Nat Med*. 2018;24(8):1108-1112. doi:10.1038/s41591-018-0089-4
2. Pappalardo Z, Gambhir Chopra D, Hennings TG, et al. A Whole-Genome RNA Interference Screen Reveals a Role for Spry2 in Insulin Transcription and the Unfolded Protein Response. *Diabetes*. 2017;66(6):1703-1712. doi:10.2337/db16-0962
3. Lee J, Pappalardo Z, Chopra DG, et al. A Genetic Interaction Map of Insulin Production Identifies Mfi as an Inhibitor of Mitochondrial Fission. *Endocrinology*. 2018;159(9):3321-3330. doi:10.1210/en.2018-00426
4. Mishra P, Chan DC. Metabolic regulation of mitochondrial dynamics. *J Cell Biol*. 2016;212(4):379-387. doi:10.1083/jcb.201511036
5. Lee JE, Westrate LM, Wu H, Page C, Voeltz GK. Multiple dynamin family members collaborate to drive mitochondrial division. *Nature*. 2016;540(7631):139-143. doi:10.1038/nature20555
6. Reinhardt F, Schultz J, Waterstradt R, Baltrusch S. Drp1 guarding of the mitochondrial network is important for glucose-stimulated insulin secretion in pancreatic beta cells. *Biochem Biophys Res Commun*. 2016;474(4):646-651. doi:10.1016/j.bbrc.2016.04.142
7. Kabra UD, Pfuhlmann K, Migliorini A, et al. Direct substrate delivery into mitochondrial fission-deficient pancreatic islets rescues insulin secretion. *Diabetes*. 2017;66(5):1247-1257. doi:10.2337/db16-1088
8. Jhun BS, Lee H, Jin Z-G, Yoon Y. Glucose stimulation induces dynamic change of mitochondrial morphology to promote insulin secretion in the insulinoma cell line INS-1E. *PLoS One*. 2013;8(4):e60810. doi:10.1371/journal.pone.0060810
9. Henquin JC. Triggering and amplifying pathways of regulation of insulin secretion by glucose. *Diabetes*. 2000;49(11):1751-1760. doi:10.2337/diabetes.49.11.1751
10. Henquin JC. The dual control of insulin secretion by glucose involves triggering and amplifying pathways in β-cells. *Diabetes Res Clin Pract*. 2011;93(SUPPL. 1):S27-S31.

doi:10.1016/S0168-8227(11)70010-9

11. Kalwat MA, Cobb MH. Mechanisms of the amplifying pathway of insulin secretion in the β cell. *Pharmacol Ther*. 2017;179:17-30. doi:10.1016/j.pharmthera.2017.05.003
12. Maechler P. Mitochondrial function and insulin secretion. *Mol Cell Endocrinol*. 2013;379(1-2):12-18. doi:10.1016/j.mce.2013.06.019
13. Zhang Z, Wakabayashi N, Wakabayashi J, et al. The dynamin-related GTPase Opa1 is required for glucose-stimulated ATP production in pancreatic beta cells. *Mol Biol Cell*. 2011;22(13):2235-2245. doi:10.1091/mbc.E10-12-0933
14. Supale S, Thorel F, Merkwirth C, et al. Loss of prohibitin induces mitochondrial damages altering β-cell function and survival and is responsible for gradual diabetes development. *Diabetes*. 2013;62(10):3488-3499. doi:10.2337/db13-0152
15. Bordt EA, Clerc P, Roelofs BA, et al. The Putative Drp1 Inhibitor mdivi-1 Is a Reversible Mitochondrial Complex I Inhibitor that Modulates Reactive Oxygen Species. *Dev Cell*. 2017;40(6):583-594.e6. doi:10.1016/j.devcel.2017.02.020
16. Wakabayashi J, Zhang Z, Wakabayashi N, et al. The dynamin-related GTPase Drp1 is required for embryonic and brain development in mice. *J Cell Biol*. 2009;186(6):805-816. doi:10.1083/jcb.200903065
17. Thorens B, Tarussio D, Maestro MA, Rovira M, Heikkilä E, Ferrer J. Ins1(Cre) knock-in mice for beta cell-specific gene recombination. *Diabetologia*. 2015;58(3):558-565. doi:10.1007/s00125-014-3468-5
18. Opaliński Ł, Veenhuis M, van der Klei IJ. Peroxisomes: membrane events accompanying peroxisome proliferation. *Int J Biochem Cell Biol*. 2011;43(6):847-851. doi:10.1016/j.biocel.2011.03.006
19. Schrader M. Shared components of mitochondrial and peroxisomal division. *Biochim Biophys Acta*. 2006;1763(5-6):531-541. doi:10.1016/j.bbamcr.2006.01.004
20. Koch A, Thiemann M, Grabenbauer M, Yoon Y, McNiven MA, Schrader M. Dynamin-like

protein 1 is involved in peroxisomal fission. *J Biol Chem*. 2003;278(10):8597-8605. doi:10.1074/jbc.M211761200

21. Ban-Ishihara R, Ishihara T, Sasaki N, Mihara K, Ishihara N. Dynamics of nucleoid structure regulated by mitochondrial fission contributes to cristae reformation and release of cytochrome c. *Proc Natl Acad Sci*. 2013;110(29):11863-11868. doi:10.1073/pnas.1301951110
22. Ishihara T, Ban-Ishihara R, Maeda M, et al. Dynamics of mitochondrial DNA nucleoids regulated by mitochondrial fission is essential for maintenance of homogeneously active mitochondria during neonatal heart development. *Mol Cell Biol*. 2015;35(1):211-223. doi:10.1128/MCB.01054-14
23. Patterson GH, Knobel SM, Arkhammar P, Thastrup O, Piston DW. Separation of the glucose-stimulated cytoplasmic and mitochondrial NAD(P)H responses in pancreatic islet beta cells. *Proc Natl Acad Sci U S A*. 2000;97(10):5203-5207. doi:10.1073/pnas.090098797
24. Gregg T, Poudel C, Schmidt BA, et al. Pancreatic β-cells from mice offset age-associated mitochondrial deficiency with reduced KATP channel activity. *Diabetes*. 2016;65(9):2700-2710. doi:10.2337/db16-0432
25. Ravier MA, Daro D, Roma LP, et al. Mechanisms of control of the free Ca2+ concentration in the endoplasmic reticulum of mouse pancreatic β-cells: interplay with cell metabolism and [Ca2+]c and role of SERCA2b and SERCA3. *Diabetes*. 2011;60(10):2533-2545. doi:10.2337/db10-1543
26. Henquin JC. Regulation of insulin secretion: a matter of phase control and amplitude modulation. *Diabetologia*. 2009;52(5):739-751. doi:10.1007/s00125-009-1314-y
27. Brand MD, Nicholls DG. Assessing mitochondrial dysfunction in cells. *Biochem J*. 2011;435(2):297-312. doi:10.1042/BJ20110162
28. Song M, Mihara K, Chen Y, Scorrano L, Dorn GW. Mitochondrial fission and fusion

factors reciprocally orchestrate mitophagic culling in mouse hearts and cultured fibroblasts. *Cell Metab*. 2015;21(2):273-285. doi:10.1016/j.cmet.2014.12.011

29. Shields LY, Kim H, Zhu L, et al. Dynamin-related protein 1 is required for normal mitochondrial bioenergetic and synaptic function in CA1 hippocampal neurons. *Cell Death Dis*. 2015;6(4):e1725. doi:10.1038/cddis.2015.94

30. Wang Y, Subramanian M, Yurdagul A, et al. Mitochondrial Fission Promotes the Continued Clearance of Apoptotic Cells by Macrophages. *Cell*. 2017;171(2):331-345.e22. doi:10.1016/j.cell.2017.08.041

31. Ferdaoussi M, Dai X, Jensen M V, et al. Isocitrate-to-SENP1 signaling amplifies insulin secretion and rescues dysfunctional β cells. *J Clin Invest*. 2015;125(10):3847-3860. doi:10.1172/JCI82498

32. Kibbey RG, Pongratz RL, Romanelli AJ, Wollheim CB, Cline GW, Shulman GI. Mitochondrial GTP regulates glucose-stimulated insulin secretion. *Cell Metab*. 2007;5(4):253-264. doi:10.1016/j.cmet.2007.02.008

33. Montemurro C, Vadrevu S, Gurlo T, et al. Cell cycle-related metabolism and mitochondrial dynamics in a replication-competent pancreatic beta-cell line. *Cell Cycle*. 2017;4101(August):1-14. doi:10.1080/15384101.2017.1361069

34. Düfer M, Krippeit-Drews P, Buntinas L, Siemen D, Drews G. Methyl pyruvate stimulates pancreatic beta-cells by a direct effect on KATP channels, and not as a mitochondrial substrate. *Biochem J*. 2002;368(Pt 3):817-825. doi:10.1042/BJ20020657

35. Ikeda Y, Shirakabe A, Maejima Y, et al. Endogenous Drp1 mediates mitochondrial autophagy and protects the heart against energy stress. *Circ Res*. 2015;116(2):264-278. doi:10.1161/CIRCRESAHA.116.303356

36. Shirakabe A, Zhai P, Ikeda Y, et al. Drp1-Dependent Mitochondrial Autophagy Plays a Protective Role Against Pressure Overload-Induced Mitochondrial Dysfunction and Heart Failure. *Circulation*. 2016;133(13):1249-1263.

doi:10.1161/CIRCULATIONAHA.115.020502

37. Manczak M, Sesaki H, Kageyama Y, Reddy PH. Dynamin-related protein 1 heterozygote knockout mice do not have synaptic and mitochondrial deficiencies. *Biochim Biophys Acta*. 2012;1822(6):862-874. doi:10.1016/j.bbadis.2012.02.017

38. Kuznetsov A V., Hermann M, Saks V, Hengster P, Margreiter R. The cell-type specificity of mitochondrial dynamics. *Int J Biochem Cell Biol*. 2009;41(10):1928-1939. doi:10.1016/j.biocel.2009.03.007

39. Fergusson G, Ethier M, Guévremont M, et al. Defective insulin secretory response to intravenous glucose in C57Bl/6J compared to C57Bl/6N mice. *Mol Metab*. 2014;3(9):848-854. doi:10.1016/j.molmet.2014.09.006

40. Szot GL, Koudria P, Bluestone JA. Murine pancreatic islet isolation. *J Vis Exp*. 2007;(7):255. doi:10.3791/255

41. Schindelin J, Rueden CT, Hiner MC, Eliceiri KW. The ImageJ ecosystem: An open platform for biomedical image analysis. *Mol Reprod Dev*. 2015;82(7-8):518-529. doi:10.1002/mrd.22489

42. Kulkarni RN, Mizrachi E-B, Ocana AG, Stewart AF. Human β-cell proliferation and intracellular signaling: driving in the dark without a road map. *Diabetes*. 2012;61(9):2205-2213. doi:10.2337/db12-0018

43. Agathocleous M, Harris WA. Metabolism in physiological cell proliferation and differentiation. *Trends Cell Biol*. 2013;23(10):484-492. doi:10.1016/j.tcb.2013.05.004

44. Puri S, Roy N, Russ HA, et al. Replication confers β cell immaturity. *Nat Commun*. 2018;9(1):485. doi:10.1038/s41467-018-02939-0

45. Gutierrez GD, Gromada J, Sussel L. Heterogeneity of the Pancreatic Beta Cell. *Front Genet*. 2017;8:22. doi:10.3389/fgene.2017.00022

46. Aamodt KI, Powers AC. Signals in the pancreatic islet microenvironment influence β-cell proliferation. *Diabetes Obes Metab*. 2017;19 Suppl 1:124-136. doi:10.1111/dom.13031

47. Mayers JR, Vander Heiden MG. Famine versus feast: understanding the metabolism of tumors in vivo. *Trends Biochem Sci*. 2015;40(3):130-140. doi:10.1016/j.tibs.2015.01.004

48. Davidson SM, Papagiannakopoulos T, Olenchock BA, et al. Environment Impacts the Metabolic Dependencies of Ras-Driven Non-Small Cell Lung Cancer. *Cell Metab*. 2016;23(3):517-528. doi:10.1016/j.cmet.2016.01.007

49. Prentki M, Matschinsky FM, Madiraju SRM. Metabolic signaling in fuel-induced insulin secretion. *Cell Metab*. 2013;18(2):162-185. doi:10.1016/j.cmet.2013.05.018

50. Grespan E, Giorgino T, Arslanian S, Natali A, Ferrannini E, Mari A. *Defective Amplifying Pathway of β-Cell Secretory Response to Glucose in Type Running Head: Integrated in Vitro & in Vivo β-Cell Modeling*.; 2017.

51. Li H, Alavian KN, Lazrove E, et al. A Bcl-xL-Drp1 complex regulates synaptic vesicle membrane dynamics during endocytosis. *Nat Cell Biol*. 2013;15(7):773-785. doi:10.1038/ncb2791

52. Han Y-E, Chun JN, Kwon MJ, et al. Endocytosis of K ATP Channels Drives Glucose-Stimulated Excitation of Pancreatic β Cells. *Cell Rep*. 2018;22(2):471-481. doi:10.1016/j.celrep.2017.12.049

53. Chen H, Ren S, Clish C, et al. Titration of mitochondrial fusion rescues Mff-deficient cardiomyopathy. *J Cell Biol*. 2015;211(4):795-805. doi:10.1083/jcb.201507035

54. Burté F, Carelli V, Chinnery PF, Yu-Wai-Man P. Disturbed mitochondrial dynamics and neurodegenerative disorders. *Nat Rev Neurol*. 2015;11(1):11-24. doi:10.1038/nrneurol.2014.228

55. Sebastián D, Palacín M, Zorzano A. Mitochondrial Dynamics: Coupling Mitochondrial Fitness with Healthy Aging. *Trends Mol Med*. 2017;23(3):201-215. doi:10.1016/j.molmed.2017.01.003

56. Itoh K, Nakamura K, Iijima M, Sesaki H. Mitochondrial dynamics in neurodegeneration. *Trends Cell Biol*. 2013;23(2):64-71. doi:10.1016/j.tcb.2012.10.006

57. Dorn GW. Mitochondrial dynamics in heart disease. *Biochim Biophys Acta - Mol Cell Res*. 2013;1833(1):233-241. doi:10.1016/j.bbamcr.2012.03.008

58. Peng L, Men X, Zhang W, et al. Dynamin-related protein 1 is implicated in endoplasmic reticulum stress-induced pancreatic β-cell apoptosis. *Int J Mol Med*. 2011;28(2):161-169. doi:10.3892/ijmm.2011.684

59. Men X, Wang H, Li M, et al. Dynamin-related protein 1 mediates high glucose induced pancreatic beta cell apoptosis. *Int J Biochem Cell Biol*. 2009;41(4):879-890. doi:10.1016/j.biocel.2008.08.031

60. Peng L, Men X, Zhang W, et al. Involvement of dynamin-related protein 1 in free fatty acid-induced INS-1-derived cell apoptosis. *PLoS One*. 2012;7(11):e49258. doi:10.1371/journal.pone.0049258

61. Liu J, Chen Z, Zhang Y, et al. Rhein protects pancreatic β-cells from dynamin-related protein-1-mediated mitochondrial fission and cell apoptosis under hyperglycemia. *Diabetes*. 2013;62(11):3927-3935. doi:10.2337/db13-0251

62. Molina AJ a, Wikstrom JD, Stiles L, et al. Mitochondrial networking protects beta-cells from nutrient-induced apoptosis. *Diabetes*. 2009;58(10):2303-2315. doi:10.2337/db07-1781

63. Anello M, Lupi R, Spampinato D, et al. Functional and morphological alterations of mitochondria in pancreatic beta cells from type 2 diabetic patients. *Diabetologia*. 2005;48(2):282-289. doi:10.1007/s00125-004-1627-9

64. Dlasková A, Špaček T, Šantorová J, et al. 4Pi microscopy reveals an impaired three-dimensional mitochondrial network of pancreatic islet β-cells, an experimental model of type-2 diabetes. *Biochim Biophys Acta - Bioenerg*. 2010;1797(6-7):1327-1341. doi:10.1016/j.bbabio.2010.02.003

65. Lundberg M, Stenwall A, Tegehall A, Korsgren O, Skog O. Expression profiles of stress-related genes in islets from donors with progressively impaired glucose metabolism.

Islets. 2018;10(2):69-79. doi:10.1080/19382014.2018.1433980

66. Rocha AG, Franco A, Krezel AM, et al. MFN2 agonists reverse mitochondrial defects in preclinical models of Charcot-Marie-Tooth disease type 2A. *Science*. 2018;360(6386):336-341. doi:10.1126/science.aao1785

67. Macia E, Ehrlich M, Massol R, Boucrot E, Brunner C, Kirchhausen T. Dynasore, a cell-permeable inhibitor of dynamin. *Dev Cell*. 2006;10(6):839-850. doi:10.1016/j.devcel.2006.04.002

68. Qi X, Qvit N, Su Y-C, Mochly-Rosen D. A novel Drp1 inhibitor diminishes aberrant mitochondrial fission and neurotoxicity. *J Cell Sci*. 2013;126(Pt 3):789-802. doi:10.1242/jcs.114439

69. Cassidy-Stone A, Chipuk JE, Ingerman E, et al. Chemical inhibition of the mitochondrial division dynamin reveals its role in Bax/Bak-dependent mitochondrial outer membrane permeabilization. *Dev Cell*. 2008;14(2):193-204. doi:10.1016/j.devcel.2007.11.019

Publishing Agreement

It is the policy of the University to encourage the distribution of all theses, dissertations, and manuscripts. Copies of all UCSF theses, dissertations, and manuscripts will be routed to the library via the Graduate Division. The library will make all theses, dissertations, and manuscripts accessible to the public and will preserve these to the best of their abilities, in perpetuity.

Please sign the following statement:

I hereby grant permission to the Graduate Division of the University of California, San Francisco to release copies of my thesis, dissertation, or manuscript to the Campus Library to provide access and preservation, in whole or in part, in perpetuity.

Author Signature

12/14/18
Date